Constitutive Activation of the Canonical NF-κB Pathway Leads to Bone Marrow Failure and Induction of Erythroid Signature in Hematopoietic Stem Cells

Masahiro Marshall Nakagawa[1], **Chozha Vendan Rathinam**[1,2,3,4,5,*]

[1]Department of Genetics and Development, Columbia University Medical Center, 701 W. 168th Street, New York, NY 10032, USA

[2]Institute of Human Virology, University of Maryland, Baltimore, MD, USA

[3]Center for Stem Cell & Regenerative Medicine, University of Maryland, Baltimore, MD, USA

[4]Marlene and Stewart Greenebaum Comprehensive Cancer Center, University of Maryland School of Medicine, 725 W. Lombard Street, Baltimore, MD 21201, USA

[5]Lead Contact

SUMMARY

Constitutive activation of the canonical NF-κB pathway has been associated with a variety of human pathologies. However, molecular mechanisms through which canonical NF-κB affects hematopoiesis remain elusive. Here, we demonstrate that deregulated canonical NF-κB signals in hematopoietic stem cells (HSCs) cause a complete depletion of HSC pool, pancytopenia, bone marrow failure, and premature death. Constitutive activation of IKK2 in HSCs leads to impaired quiescence and loss of function. Gene set enrichment analysis (GSEA) identified an induction of "erythroid signature" in HSCs with augmented NF-κB activity. Mechanistic studies indicated a reduction of thrombopoietin (TPO)-mediated signals and its downstream target *p57* in HSCs, due to reduced *c-Mpl* expression in a cell-intrinsic manner. Molecular studies established Klf1 as a key suppressor of *c-Mpl* in HSPCs with increased NF-κB. In essence, these studies identified a previously unknown mechanism through which exaggerated canonical NF-κB signals affect HSCs and cause pathophysiology.

Graphical Abstract

*Correspondence: crathinam@ihv.umaryland.edu.

AUTHOR CONTRIBUTIONS

M.M.N performed the research, collected and interpreted the data, and wrote the manuscript. C.V.R. designed and performed the research, collected and interpreted the data, and wrote the manuscript.

SUPPLEMENTAL INFORMATION

Supplemental Information includes five figures and three tables and can be found with this article online at https://doi.org/10.1016/j.celrep.2018.10.071.

DECLARATION OF INTERESTS

The authors declare no competing interests.
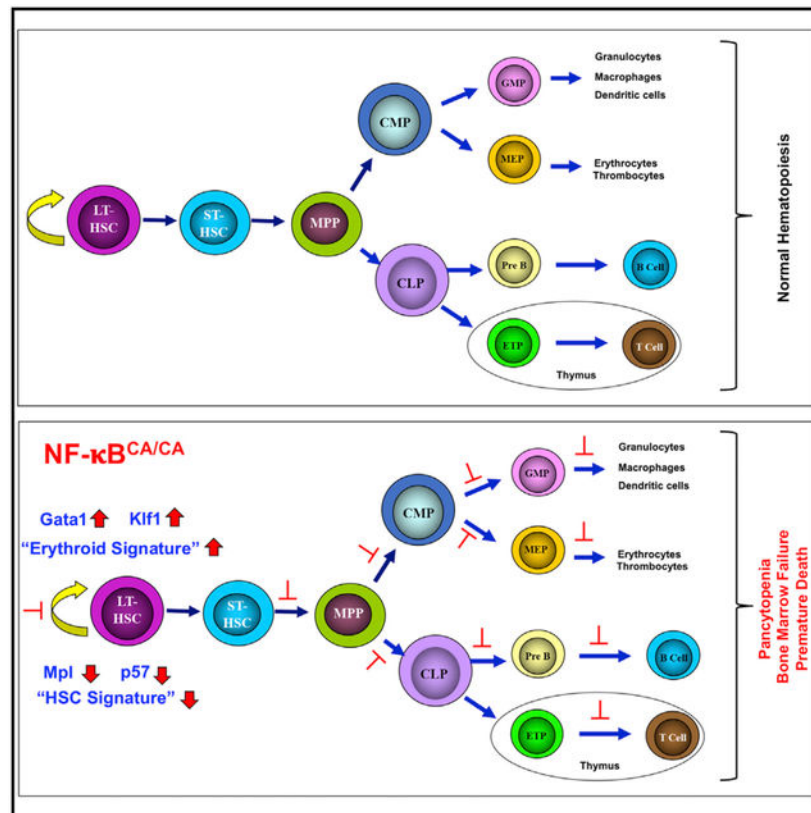
In Brief

Nakagawa and Rathinam demonstrate that constitutive activation of IKK2 in HSCs causes a complete depletion of the HSC pool and impairs HSC functions due to a loss of "sternness" signature and an induction of erythroid signature.

INTRODUCTION

Hematopoietic stem cells (HSCs) have a unique capacity to self-renew and to differentiate into all cells of the hematopoietic system (Kondo et al., 2003). In general, adult HSCs are considered slow cycling (Cheshier et al., 1999; Morrison and Weissman, 1994; Passegue et al., 2005; Yamazaki and Nakauchi, 2009) and are believed to undergo only ~18 divisions during their lifetime. Under steady-state conditions, HSCs exist in a dormant or quiescent state, and in response to external stimuli, they rapidly switch to an active or proliferative state (Trumpp et al., 2010; Wilson et al., 2008). Dormant HSCs divide once every 145–193 days and activated HSCs divide once every 28–36 days (van der Wath et al., 2009; Wilson et al., 2008).

Maintenance of quiescence has been believed to be integral to the functions of HSCs, since the capacity to reconstitute the hematopoietic system following serial transplantation was found to be contributed exclusively by quiescent HSCs (Foudi et al., 2009; Wilson et al., 2008; Wilson and Trumpp, 2006). The decision of maintaining a quiescent state or an actively proliferating state of HSCs is governed by both cell-intrinsic and -extrinsic

regulatory circuits (Kiel and Morrison, 2008; Trumpp et al., 2010; Wilson and Trumpp, 2006). Treatment of HSCs with cytokines such as granulocyte colony-stimulating factor (GCSF), interferon α (IFNα), and IFNγ activate dormant HSCs to enter the cycle, and cytokines such as stem cell factor (SCF), thrombopoietin (TPO), transforming growth factor β (TGFβ), and C-X-C motif ligand 12 (CXCL12) induce and maintain HSC quiescence (Kiel and Morrison, 2008; Trumpp et al., 2010; Wilson and Trumpp, 2006). In addition to these cell-extrinsic signals, a number of cell-intrinsic factors, including cell-cycle regulators p21 and p57, transcription factors Gfi1, EGR1, FOXOs, and PBX1, and E3 ubiquitin ligases c-Cbl, Itch, and Fbxw7, have been demonstrated to be critical for the maintenance of HSC quiescence (King et al., 2013; Orford and Scadden, 2008; Pietras et al., 2011; Rathinam et al., 2008, 2011; Trumpp et al., 2010; Zou et al., 2011).

The Rel/nuclear factor κB (NF-κB) transcription factor family of proteins function as a master regulator of genes that control innate and adaptive immunity (Vallabhapurapu and Karin, 2009). They comprise five mammalian family members: Rel A (p65), Rel B, c-Rel, p50/p105 (also known as NF-κB1), and p100/52 (also known as NF-κB2) (Ghosh and Hayden, 2008). These proteins have an N-terminal Rel homology domain (RHD) for the formation of homodimers and heterodimers of family members and for sequence-specific DNA binding. Depending upon the type of activation and members involved in the signaling cascades, NF-κB signaling has been divided broadly into canonical and non-canonical pathways. According to the current model of canonical pathway, in the absence of any specific stimulus, the inhibitor of NF-κB (IκB) proteins sequester the inactive NF-κB proteins in the cytoplasm. In response to stimulation, the IκB kinase (IKK) complex phosphorylates IκB, which leads to ubiquitylation and subsequent degradation of IκB. Following this, NF-κB complexes are released from the cytoplasm and enter the nucleus to drive the expression of target genes (Ghosh and Hayden, 2008). Thus, activation of the IKK complex is a key regulatory event in the NF-κB signal transduction pathway. IKK consists of two catalytic subunits, IKKα (also known as IKK1) and IKKβ (also known as IKK2), and the regulatory subunit IKKγ (also known as NEMO) (Rothwarf et al., 1998; Yamaoka et al., 1998; Zandi et al., 1997). IKK phosphorylates IκB proteins at two amino (N)-terminal regulatory serine residues (Brown et al., 1995). In the majority of the canonical signaling pathways, IKK2 is necessary and sufficient for the phosphorylation of IκB (Ghosh and Hayden, 2008).

Even though biochemistry and molecular functions of NF-κB have been well characterized, its precise role in hematopoiesis remains incompletely understood. In particular, the contribution of NF-κB pathways to HSC self-renewal and quiescence needs to be explored. In the present study, we attempted to define the role of NF-κB-mediated signaling events in HSC quiescence through a gain-of-function approach. Our data indicate that NF-κB signaling plays a key role in the determination of the quiescence versus the active state of HSCs and that constitutive activation of NF-κB in HSCs leads to pancytopenia and bone marrow failure.

RESULTS

Deregulated IKK2 Activation in HSCs Leads to Pancytopenia and Progressive Bone Marrow Failure

To investigate the role of the canonical NF-κB pathway in hematopoiesis, we made use of the R26Stop^{FL}IKK2ca transgenic mice, which were generated and described earlier (Sasaki et al., 2006). IKK2 containing serine to glutamate mutations (IKK2^{CA}) is constitutively active and therefore results in augmented activation and nuclear translocation of the canonical NF-κB subunit p65 (Mercurio et al., 1997). We crossed the IKK2^{CA} mice with transgenic mice that express Cre under the *Vav1* promoter to obtain IKK2$^{CA/CA}$Vav$^{Cre/+}$ (henceforth referred to as CA/CA) mice. The *Vav1* promoter has been proven to be largely specific to the hematopoietic lineage; in particular, it has been expressed at all stages of hematopoiesis—from HSCs to terminally differentiated myeloid, erythroid, and lymphoid lineage cells (Almarza et al., 2004; de Boer et al., 2003). Analysis of CA/CA mice indicated EGFP expression in the majority of the cells from bone marrow (BM), spleen, and thymus, but is absent in non-hematopoietic organs (brain, heart, lung, kidney, and liver) (Figure S1A), suggesting that the constitutively active IKK2 is expressed exclusively in the cells of the hematopoietic system. As expected, EGFP expression was detected in almost all cells of the hematopoietic stem and progenitor cell (HSPC; lineage$^-$ Sca1$^+$ c-Kit$^+$ [LSK]) subsets, including long-term HSCs (LT-HSCs; CD150$^+$CD48$^-$LSK), short-term HSCs (ST-HSCs; CD34$^+$Flt3$^-$LSK), and multipotent progenitors (MPPs; CD34$^+$Flt3$^+$LSK) (Figure S1B). Gene expression studies confirmed that NF-κB activity was augmented in both total BM (Figure 1A) and HSCs (Figure 1B) of CA/CA mice. Even though the body size of CA/CA mice was comparable with control litter-mates at 2 weeks of age, they exhibited a significant growth retardation at 4 weeks of age (Figure 1C), and almost all CA/CA mice died within 5 weeks of age (Figure 1D). To investigate the cause of their death, we performed complete blood count (CBC) analysis, which indicated progressive pancytopenia (Figure 1E) in CA/CA mice. Consistent with the CBC data, CA/CA mice showed progressive atrophy of hematopoietic organs, such as BM, spleen, and thymus (Figures 1F and 1G). These data indicated that constitutive activation of canonical NF-κB in HSCs results in progressive, fatal BM failure.

Uncontrolled NF-κB Activation Causes Premature Depletion of HSC Pool

To explore the cellular mechanisms that lead to progressive BM failure, we analyzed the HSPC compartment in the BM of CA/CA mice. HSPCs were almost absent in the BM of CA/CA mice at 4 weeks of age (Figures 2A and 2B). Instead, the frequency of lineage$^-$ Sca1$^+$ c-Kit^{low} (LSK^{low}) cells was significantly increased in CA/CA BM (Figures 2A and 2B). Of note, absolute numbers of LSK^{low} cells were not increased in CA/CA mice (Figure 2B) due to a striking decrease in cellularity of the BM from CA/CA mice (Figure 1H). To find a direct correlation between pancytopenia and loss of HSC pool, we analyzed HSPCs from 2-week-old CA/CA mice, as white blood cell (WBC) counts and cellularity of hematopoietic organs were not decreased at that stage. While overall LSK cell numbers were not reduced, LT-HSCs were diminished (4.8% versus 0.03%), ST-HSCs were increased (34% versus 83%), and MPPs were significantly reduced (61% versus 7%) in the BM of 2-week-old CA/CA mice (Figures 2C and 2D). To independently validate our findings through

an alternative and a more refined immunophenotyping scheme of HSPCs, we followed the surface staining strategy that was established earlier (Wilson et al., 2008). Accordingly, the frequencies of HSC (CD34$^-$Flt3$^-$CD48$^-$CD150$^+$ LSK cells) and multipotent progenitor 1 (MPP1; CD34$^+$Flt3$^-$CD48$^-$CD150$^+$ LSK cells) were completely absent, multipotent progenitor 2 (MPP2; CD34$^+$Flt3$^-$CD48$^+$CD150$^+$ LSK cells) and multipotent progenitor 3 (MPP3; CD34$^+$Flt3$^-$CD48$^+$CD150$^-$ LSK cells) were remarkably increased, and multipotent progenitor 4 (MPP4; CD34$^+$Flt3$^+$CD48$^+$CD150$^-$ LSK cells) were significantly decreased (Figures 2E and 2F) in the BM of 2-week-old CA/CA mice. Because HSCs were remarkably reduced in the BM of CA/CA mice as early as 2 weeks after birth, we focused on fetal hematopoiesis to assess whether HSC defects could be observed during fetal development. Even though overall HSPCs (LSK) and ST-HSCs were increased in CA/CA fetal liver (embryonic day [E]18), LT-HSCs were remarkably decreased during fetal hematopoiesis (Figures 2G and 2H). Of note, the total numbers of MPPs were not altered during fetal hematopoiesis (Figures 2G and 2H).

To study the impact of constitutive NF-κB activation in adult HSCs, we generated an inducible IKK2$^{F/F}$Mx1$^{cre/+}$ mouse model. IKK2$^{F/F}$Mx1$^{cre/+}$ and control mice 4 to 6 weeks old were injected with three doses of polyI:C (250 μg/mouse) every other day to induce constitutive activation of IKK2. After 3–4 weeks, Mx1 Cre-mediated recombination was confirmed based on GFP expression and genomic PCR in HSPCs and BM cells (data not shown). An analysis of the HSPC compartment of IKK2$^{F/F}$ Mx1$^{cre/+}$ mice indicated increased numbers of LSK cells; highly reduced numbers of LT-HSC pool, MPP1, and MPP4; and increased numbers of MPP2 and MPP3 (Figures 2I and 2J). Thus, the data of IKK2$^{F/F}$Mx1$^{cre/+}$ mice corroborate the results obtained using CA/CA mice. Overall, these results provide evidence that constitutive activation of NF-κB depletes the HSC pool and affects selective differentiation of MPP subsets, which may be responsible for the progressive and fatal BM failure in CA/CA mice.

Constitutive Activation of NF-κB Affects HSC Functions and Quiescence

Even though immunophenotyping studies indicated a severe reduction of HSC pool in CA/CA mice, it remains possible that the functional HSCs are not affected in these mice. To evaluate the functions of HSCs, we performed BM transplantation (BMT) assays. We transplanted red blood cell (RBC)-depleted total BM from 2-week-old (because LSK cells are not decreased in CA/CA BM at this time point) CA/CA and control mice into lethally irradiated wild-type recipients. As shown in Figure 3A, all of the recipients that received BM from CA/CA mice died within 3 weeks of transplantation, indicating that CA/CA BM lacks functional HSCs. To overcome the lethal phenotype observed in CA/CA recipients and to provide favorable conditions in which CA/CA HSCs may contribute to donor hematopoiesis, in spite of their compromised functions, we performed mixed BM chimera experiments. Donor (CD45.2$^+$) BM cells (either CA/CA or control) were mixed with wild-type BM (CD45.1$^+$) cells in 1:1, 3:1, and 5:1 ratios and transplanted into lethally irradiated wild-type (CD45.1$^+$) recipients. An analysis of recipients revealed an absence of CA/CA-derived hematopoiesis as early as 4 weeks of transplantation, even at a (CA/CA: wild-type) ratio of 5:1 (Figures 3B, S1C, and S1D). These data suggest that although LSK cells are not decreased in CA/CA mice at 2 weeks of age, the functional HSCs are almost absent in their

BM. We performed similar BMT experiments using adult BM from polyI:C-injected IKK2$^{F/F}$Mx1$^{cre/+}$ mice, and the results of these studies were consistent with the data obtained from the BM of CA/CA mice (Figure 3C). To identify the cell-intrinsic role of constitutively active IKK2 in HSC maintenance and functions, we performed a series of BMT experiments. We transferred either total BM of IKK2$^{F/F}$Mx1$^{cre/+}$ mice or mixed BM (IKK2$^{F/F}$Mx1$^{cre/+}$ [CD45.2$^+$] + wild-type [WT] [CD45.1$^+$] BM cells at a ratio of 1:1) into lethally irradiated CD45.1 WT recipients. After 4 weeks of BMT, polyI:C was injected into recipients to activate IKK2 specifically in hematopoietic cells. Consistent with the data shown in Figure 3C, all of the recipients that received total BM of IKK2$^{F/F}$Mx1$^{cre/+}$ mice died within 30 days of transplantation (Figure 3D). Peripheral blood analysis of recipients that received total BM of IKK2$^{F/F}$Mx1$^{cre/+}$ mice indicated a severe reduction in donor-derived hematopoiesis at 2 weeks after transplantation (Figure 3E). In keeping with these results, an analysis of recipients that received mixed BM revealed a striking reduction in IKK2$^{F/F}$Mx1$^{cre/+}$ (CD45.2$^+$)-derived hematopoiesis at 4 weeks of transplantation (Figure 3F). To unequivocally demonstrate that the hematopoietic phenotype of CA/CA mice was not caused by defective niche signals, we performed reciprocal BMT studies. Total BM cells from congenic (CD45.1$^+$) WT mice were injected into lethally irradiated either control or IKK2$^{F/F}$Mx1$^{cre/+}$ mice, and 4 weeks after transplantation, recipients were injected with polyI:C to induce recombination. Nine of 10 IKK2$^{F/F}$Mx1$^{cre/+}$ recipients survived throughout the observed period of 75 days (Figure 3G), and an analysis of peripheral blood at 8 weeks of transplantation indicated comparable levels of donor-derived hematopoiesis in control and IKK2$^{F/F}$Mx1$^{cre/+}$ recipients (Figure 3H). These data strongly indicate that constitutive activation of IKK2 affects HSC functions in a cell-intrinsic manner.

To identify the cellular mechanisms leading to the loss of the HSC pool of CA/CA mice, first, we performed apoptosis studies. Our data indicated that apoptosis of either total BM cells or LSK cells was slightly increased in CA/CA mice when compared with control BM (Figures S2A and S2B). Second, we analyzed the cell-cycle status of HSPCs, and the data revealed that the most quiescent G0 (Ki67$^-$ and Hoechst$^-$) cells were decreased, whereas cells in G2/S phase were remarkably increased in both total LSK and Flt3^{low}LSK subsets in the BM of CA/CA mice (Figures 3I and 3J). Further analysis indicated an increase (2% in control versus 30% in CA/CA) of a highly proliferating fraction (Ki67^{high}) of cells within the Flt3^{low}LSK compartment of CA/CA mice (Figures 3K and 3L). Because LT-HSCs were almost absent in CA/CA mice as early as 2 weeks of age, it was technically difficult to directly assess the proliferation status of LT-HSCs. To overcome this challenge, we performed BrdU labeling experiments with fetal liver (E18) HSCs, as we described earlier (Nakagawa et al., 2015). While the proliferation of total LSK cells was slightly increased (71% in control versus 82% in CA/CA), the frequencies of proliferating LT-HSCs were greatly increased (38% in control and 57% in CA/CA) in the liver of CA/CA fetuses (Figures 3M and 3N). Overall, these data indicate that constitutive activation of IKK2 leads to the loss of HSC functions and quiescence.

Augmented NF-κB Activation Results in Loss of the Molecular Signature of HSCs

NF-κκB has been shown to play an indispensable role in the secretion of pro-inflammatory cytokines by the effector cells of the immune system (Ghosh and Hayden, 2008; Karin,

2006; Vallabhapurapu and Karin, 2009). We have previously shown that deregulated NF-κB signals (in A20[Hem-KO] [knockout] mice) led to increased levels of pro-inflammatory cytokines, such as tumor necrosis factor α (TNFα), interleukin 1β (IL1β), IL6, and IFNγ in the BM and spleen, and that augmented IFNγ signaling was largely responsible for the loss of HSC pool and functions of A20[Hem-KO] mice (Nakagawa et al., 2015). Deregulated signaling mediated by both type 1 and type 2 INFs causes loss of quiescence and functions of HSC (Baldridge et al., 2010; de Bruin et al., 2014; Essers et al., 2009; King et al., 2011). Based on these findings, we investigated the role of inflammatory signals on the HSC phenotype of CA/CA mice. Our gene expression studies identified an elevated expression of IL1β, IL6, TNFα, and IFNγ in the BM (Figure 4A) and spleen (Figure 4B) of CA/CA mice. Even though increased levels of IL1β, IL6, TNFα, and IFNγ were observed, we primarily focused on the role of IFNγ, because our previous studies on A20[Hem-KO] mice revealed that blocking IFNγ signaling was sufficient to rescue the HSC phenotype (Nakagawa et al., 2015). Hence, we crossed the CA mice with IFNγ$^{-/-}$ mice and our analysis revealed that, unlike in A20[Hem-KO] mice, blocking IFNγ signals could not rescue the phenotype of CA mice (data not shown), suggesting that the HSC defects of CA/CA mice may be caused by some other mechanisms. To gain insights into molecular mechanisms through which NF-κB affects HSC quiescence and functions, we performed genome-wide transcriptional profiling assays using ST-HSCs (Flt3^{low} LSK cells), because LTHSCs were almost absent in IKK2 mutant mice. Our genome-wide transcriptional profiling assays revealed a differential expression (> or <1.5-fold, respectively) of 1,722 (661 upregulated and 1,061 downregulated) genes in CA/CA HSCs when compared with control HSCs (Table S1). To understand potential upstream regulators or pathways that may be associated with the constitutive activation of IKK2, we performed Gene Ontology (GO) analysis. The top 200 genes from the list of upregulated genes and bottom 200 genes from the list of downregulated genes in CA/CA HSCs were subjected to GO analysis. Results of this analysis indicated an upregulation of genes associated with diverse cellular processes such as glycerol transport, transmembrane transport, response to thyroid hormone and erythrocyte differentiation, and downregulation of genes associated with leukocyte migration, inflammatory response, myeloid cell differentiation, cell adhesion, and metabolic pathways (Table S2).

To identify specific gene sets that were deregulated in CA/CA HSCs, we performed gene set enrichment analysis (GSEA) and compared the gene expression profiles of CA/CA HSCs with previously reported stem cell-associated gene sets. First, we used "stemness"-related gene sets, which were commonly upregulated in HSCs, muscle stem cells (MuSCs), and hair follicle stem cells (HFSCs) (Cheung and Rando, 2013), and this signature was significantly downregulated in CA/CA HSCs but was enriched in control HSCs (Figure 4C; Table S3). Second, we compared our data with the genes enriched in normal, steady-state BM HSCs from WT mice compared to MPPs, leukemic stem cells (LSCs), and mobilized HSCs (Forsberg et al., 2010). As shown in Figure 4D and Table S3, this HSC signature was highly enriched in control HSCs but downregulated in CA/CA HSCs. Third, we compared our data with the genes that were commonly upregulated in adult quiescent HSCs (versus fetal liver HSCs) and 0, 1, 10, and 30 days after 5-fluorouracil (5-FU) injection (versus 2, 3, and 6 days after 5-FU injection) (Venezia et al., 2004). Again, this quiescence signature was

downregulated in CA/CA HSCs (Figure 4E; Table S3). Fourth, we compared our microarray data with gene sets that were commonly downregulated in HSCs, MuSCs, and HFSCs (Cheung and Rando, 2013) and found that this lineage signature was enriched in CA/CA HSCs (Figure 4F; Table S3). Fifth, we compared our dataset with mobilized HSC signature genes, which were enriched in day +2 mobilized HSC by cyclophosphamide/GCSF compared to HSCs at steady state (Forsberg et al., 2010). This mobilized HSC signature was enriched in CA/CA HSCs (Figure 4G; Table S3). Finally, we analyzed proliferative HSC genes, which were commonly upregulated in fetal liver HSCs (versus adult HSCs) and in HSCs on days 2, 3, and 6 after 5-FU injection (versus 0, 1, 10, and 30 days after 5-FU injection) (Venezia et al., 2004). Again, this proliferative HSC signature was enriched in CA/CA HSCs (Figure 4H; Table S3). We also compared our microarray data with the previously available datasets that were enriched in cells undergoing increased apoptosis (Subramanian et al., 2005). Consistent with our flow cytometry data, this apoptosis signature was not significantly enriched in CA/CA HSCs (Figure S2C), although Fas expression was slightly (1.37-fold to control) increased (Figure S2D). Together, our transcriptional profiling and *in silico* analyses further strengthened our findings that increased NF-κB signals perturb quiescence, favor the proliferation of HSCs, impair HSC stemness, and promote lineage differentiation.

Elevated NF-κB Signals Induce Erythroid Transcriptional Program in HSCs

To identify the lineage-specific molecular program that is induced by NF-κB in HSCs, we further expanded our GSEA studies and performed an *in silico* analysis by comparing the CA/CA HSC molecular signature with previously published molecular signatures of 38 distinct hematopoietic cell populations (Seita et al., 2012). The list of analyzed subsets includes HSC; MPP; common myeloid progenitor (CMP); granulocyte monocyte progenitor (GMP); pre-megakaryocyte/erythrocyte progenitor (pMEP); MEP; pre-colony-forming unit-erythroid (preCFU-E); megakaryocyte progenitor (MkP); common lymphoid progenitor (CLP); B-lymphoid progenitor (BLP); pre-pro B cell, B cell progenitor (fractions B–E); granulocytes and monocytes of BM; T cell progenitors (DN-DP) and CD4/CD8 T cell subsets of thymus; and B cell subsets and NK cells of spleen (Seita et al., 2012). We first compared the expression profile of each hematopoietic subset listed above with the expression profile of HSCs (Seita et al., 2012). Through this analysis, we identified the top 100 upregulated genes in each hematopoietic subset (compared to HSCs) and identified these gene sets as the typical molecular signature of each hematopoietic subset. Second, we compared each of these gene sets (from a total of 38 gene sets), with the molecular signatures of CA/CA and control HSCs that were obtained through our transcriptional profiling studies. Among the 38 populations analyzed, the molecular signatures of pMEP and MEP were (nominal p value <1%) enriched in CA/CA HSCs, but not in control HSCs (Figures 5A and 5B; Table S3). Alternatively, we generated gene sets that contained the bottom 100 genes (downregulated) in the pMEP and MEP subsets when compared with HSCs (Seita et al., 2012) and compared these gene sets with the expression data of CA/CA and control HSCs. Consistent with the previous results, these gene sets were remarkably enriched in control HSCs, but not in CA/CA HSCs (Figures S3A and S3B).

To further substantiate these results, we made a CA/CA signature gene set by selecting the top 100 upregulated genes in CA/CA HSCs when compared with control HSCs and compared this CA/CA signature gene set with previously reported expression profiles of HSCs, pMEPs, and MEPs (Seita et al., 2012). Our GSEA revealed that the CA/CA signature significantly resembled pMEP (Figure 5C; Table S3) and MEP (Figure 5D; Table S3) signatures, but not the HSC signature. Similarly, we made a gene set that contained the bottom 100 (downregulated) genes in CA/CA HSCs when compared with WT HSCs, and this gene set was significantly enriched in HSCs (Figures S3C and S3D).

To identify whether the constitutive activation of NF-κB induces the molecular signatures of both erythrocyte and megakaryocyte lineages, or of one of these two lineages in HSCs, we compared the molecular signatures of more committed progenitors of either erythroid lineage (pCFU-E) or megakaryocytic lineage (MkP) with the expression profile data of CA/CA and control HSCs. Our data indicated that the molecular signature of CA/CA HSCs resembles the pCFU-E signature (Figure 5E; Table S3), but not the MkP signature (Figure 5F; Table S3). The CA/CA signature was consistently enriched only in pCFU-E, but not in MkP (Figure 5G; Table S3). Reciprocally, the gene set that contained the bottom 100 (downregulated) genes of CA/CA HSCs was enriched in MkPs (Figure S3E). Because the CA/CA signature strongly resembled the signature of erythroid progenitors, we compared the CA/CA HSC signature with two independent erythroid lineage-related gene sets that are available in the public database. As expected, the erythrocyte differentiation signature (GO 30218) was significantly enriched in CA/CA HSCs (Figure 5H; Table S3) and the heme metabolism signature (Hallmark signature in GSEA) was also remarkably enriched in CA/CA HSCs (Figure 5I; Table S3).

To identify the functional consequences of these altered genetic signatures and erythroid-specific genetic program in HSCs, we quantified erythroid lineage committed cells by flow cytometry. The analysis revealed an increased frequency of erythroid committed progenitors, including CFU-E (Lin$^-$Sca1$^-$c-Kit$^+$CD16/32$^-$CD41$^-$CD105$^+$CD150$^-$) and pCFU-E (Lin$^-$Sca1$^-$c-Kit$^+$CD16/32$^-$CD41$^-$CD105$^+$CD150$^+$) in CA/CA BM (Figure 5J). Alternatively, the frequencies of progenitor granulocyte and macrophage (pGM; Lin$^-$Sca1$^-$c-Kit$^+$CD16/32$^-$CD41$^-$CD105$^-$CD150$^-$), progenitor megakaryocyte and erythrocyte (pMegE; Lin$^-$Sca1$^-$c-Kit$^+$ CD16/32$^-$CD41$^-$CD105$^-$CD150$^-$) (Figure 5J), and MkP (Lin$^-$Sca1$^-$c-Kit$^+$CD41$^+$CD150$^+$) (Figure 5K) were reduced in the BM of CA/CA mice. An analysis of the specific stages of erythrocyte maturation revealed a preferential increase of pro-erythrocytes (CD71$^+$Ter119$^-$) and less mature erythroblasts (TER119^{high}CD71^{high}FSC^{low}) in the BM of CA/CA mice (Figures 5L and 5M). These data provide compelling evidence that the constitutive activation of NF-κB induces an erythroid differentiation program in HSCs.

Constitutive Activation of NF-κκB Affects the Expression of p57 and c-Mpl

Our transcriptional profiling and bioinformatics studies suggested that CA/CA HSCs lack the stemness signature and acquire an erythroid lineage signature. While this may partially explain the HSC phenotype of CA/CA mice, the mechanisms that are responsible for perturbed quiescence and functions of CA/CA HSCs needed to be identified. Thus, we focused on identifying specific molecular pathways that are deregulated in CA/CA HSCs.

Among others, we focused on cell-cycle regulators, including cyclin-dependent kinases (CDKs) and CDK inhibitors (CDKIs), because defective functions of CDKs and CDKIs have been associated with defective HSC quiescence (Orford and Scadden, 2008; Pietras et al., 2011). Our bioinformatics studies identified *Cdkn1c* (*p57*) as the most affected (downregulated >2-fold) CDKI, even though modest changes in the expression of other cell-cycle regulators such as *Cdk6, Ccnh, Ccnd3, Cdk5r1,* and *Cdkn2d* were observed in CA/CA HSCs (Figure S4A). Real-time PCR studies documented a more severe reduction (~10-fold) of *p57* in Flt3⁻LSK of CA/CA mice (Figure 6A). p57 has been shown to be critical for the maintenance of quiescence in HSCs (Matsumoto et al., 2011; Tesio and Trumpp, 2011; Zou et al., 2011). Previous studies demonstrated that TPO/c-Mpl signaling pathways are essential for the expression of p57 in LT-HSCs (Qian et al., 2007; Yoshihara et al., 2007). To assess whether TPO signaling is intact in CA/CA HSCs, we stimulated cells with TPO and measured the phosphorylation levels of signal transducer and activator of transcription 5 (STAT5) through phosflow studies, because STAT5 is a key downstream target of TPO in HSCs (Kato et al., 2005). Our analysis indicated a significant decrease in the levels of phosphorylated STAT5 in CA/CA HSCs (Figure 6B). Of note, responses to either IL3 or SCF were not diminished in IKK2 mutant HSCs (Figure S4B). Based on our findings that CA/CA HSCs show reduced responses to TPO, we hypothesized that the expression of c-Mpl is reduced in CA/CA HSCs. To validate this, we quantified the surface expression levels of c-Mpl by flow cytometry. Consistent with our hypothesis, c-Mpl levels were reduced in both Flt3$^{-/low}$ LSK and Flt3$^{+/high}$ LSK fractions of CA/CA mice (Figures 6C and 6D). To assess whether the reduced surface expression of c-Mpl is due to diminished transcription, we explored our microarray data and performed real-time PCR experiments. The data of both microarray (Figure S4C) and real-time PCR indicated a remarkable decrease of *c-Mpl* mRNA in CA/CA Flt3$^{-/low}$ LSK cells (Figure 6E). To corroborate these findings and to test whether the constitutive activation of IKK2 results in reduced c-Mpl levels in adult HSCs, we analyzed the HSPCs of IKK2$^{F/F}$Mx1$^{cre/+}$ mice, following polyI:C injections. Consistent with the IKK2$^{F/F}$Vav$^{cre/+}$ model, the constitutive activation of IKK2 resulted in reduced surface expression of c-Mpl in LSK cells of IKK2$^{F/F}$Mx1$^{cre/+}$ mice (Figure 6F). Further characterization of LSK cells indicated reduced c-Mpl levels in both Flt3$^{-/low}$ LSK (Figure 6G) and Flt3$^{+/high}$ LSK (Figure 6H), even though the expression levels were more reduced in the Flt3$^{-/low}$ LSK fraction of IKK2$^{F/F}$Mx1$^{cre/+}$ mice. To further strengthen these results, we analyzed the HSPCs of A20$^{F/F}$Vav$^{cre/+}$ mice that we generated and published earlier (Nakagawa et al., 2015). Of note, A20 deficiency leads to increased NF-κB activity in HSCs (Nakagawa et al., 2015), similar to CA/CA mice. Analysis of LSK cells from A20$^{F/F}$Vav$^{cre/+}$ mice indicated a significant reduction in surface c-Mpl levels in LSK cells (Figure 6I). These results strongly indicate that the downregulation of c-Mpl is caused by constitutively activated IKK2 in a cell-intrinsic manner.

Klf1 Directly Suppresses *c-Mpl* Expression in IKK2 Mutant Hematopoietic Cells

To explore the mechanism through which *c-Mpl* is repressed and erythroid lineage transcription program is activated in CA/CA HSCs, we focused on upregulated transcription factors (TFs) (GO 0044212) in CA/CA HSCs. Among the differentially expressed TFs, Krüppel-like factor 1 (*Klf1*) (fold change 8.3) and *Gata1* (fold change 2.7) were the two most highly upregulated TFs in CA/CA HSCs (Figure S5A). We confirmed these microarray

data independently through real-time PCR assays (Figures 1D and 7A). It has been unequivocally proven that Gata1 is an essential TF for erythrocyte differentiation and expressed at very low levels, and that Gata2 is expressed at higher levels in HSCs (Bresnick et al., 2010; Suzuki et al., 2013; Takai et al., 2013). However, our analysis indicated a significant downregulation of *Gata2* (Figure 7B) and upregulation of *Gata1* (Figure 7A) in CA/CA HSCs.

Another observation that emerged from our gene expression studies was the upregulation of *Klf1* in CA/CA HSCs. Klf1 is a crucial TF for erythroid cell differentiation and is usually not expressed in HSPCs. Klf1$^{+/high}$ cells will differentiate into the erythroid lineage, while Klf1$^{-/low}$ cells will differentiate into megakaryocytic lineage cells (Figure S5B) (Starck et al., 2003). In contrast to Klf1, Gata1 is highly expressed in both erythroid and megakaryocyte lineage cells (Figure S5B) (Starck et al., 2003).

Because c-Mpl is expressed in HSCs and megakaryocyte lineage cells but absent in erythrocytes, and Klf1 is absent in in HSCs and megakaryocyte lineage cells but highly expressed in erythrocytes, we hypothesized that Klf1 directly suppresses the expression of *c-Mpl*. To validate our hypothesis, we performed an *in silico* analysis to compare the expression levels of *c-Mpl* and *Klf1* in distinct hematopoietic progenitors during differentiation of erythrocytes/megakaryocytes from HSCs, using previously published microarray data (GEO: GSE34723) (Seita et al., 2012). As shown in Figures 7C and 7D, a striking inverse correlation was found between the expression levels of *c-Mpl* and *Klf1* (p = 0.0077), especially in HSCs. However, there was no significant correlation between *Gata1* and *c-Mpl* expression during erythroid/megakaryocytic differentiation (Figures S5C and S5D). Next, we assessed whether Klf1 acts as a transcriptional repressor of *c-Mpl*. To this end, we performed bioinformatics studies to identify Klf1 binding sites in the *c-Mpl* promoter. We found three possible Klf1 binding sites in the mouse *c-Mpl* promoter region (−246 to −239, −232 to −236, and −150 to −146, from the transcription start site) and designed primers flanking this region (Figures 7E and S5E). Through chromatin immunoprecipitation (ChIP) assays, we found that Klf1 was bound to the *c-Mpl* promoter region and that the binding was greater in either total BM cells or purified Lin⁻ progenitor cells of CA/CA mice than in WT hematopoietic cells (Figure 7F). To strengthen our findings and to prove that the binding of Klf1 to the *c-Mpl* promoter results in the suppression of *c-Mpl*, we performed luciferase studies. We cloned the mouse *c-Mpl* promoter region (−496 to 19) with the Klf1 binding sites into a promoterless luciferase-expressing vector and performed the reporter assay. Consistent with our hypothesis, the presence of Klf1 significantly suppressed *c-Mpl* promoter activity (Figure 7G). Finally, to directly demonstrate the impact of *Klf1* overexpression on *c-Mpl* expression in HSPCs, we performed retroviral transduction studies. We transduced WT HSPCs (LSK cells) with retroviruses encoding for either Klf1-internal ribosome entry site (IRES)-EGFP or control IRES-EGFP. As expected, overexpression of Klf1 resulted in the reduced expression of *c-Mpl* in HSPCs (Figure 7H). These data indicate that Klf1 is a direct repressor of *c-Mpl* in HSPCs.

DISCUSSION

In the present study, we describe the consequences of increased NF-κB signals on the maintenance of HSCs. IKK2 CA/CA mice show reduced survival due to pancytopenia and BM failure as early as 4 weeks of age. Augmented NF-κB in HSCs causes a reduction in the LT-HSC pool, relative accumulation of the ST-HSC pool, and loss of Flt3$^+$ MPPs. The BM of IKK2 CA mice completely lack the c-Kit$^+$ fraction that contains all of the HSPC subsets as early as 4 weeks of age. Of note, the reduction of the LT-HSC pool has been observed in the fetal livers of 18-day-old (E18) embryos. BMT studies confirmed the absence of functional HSCs in the BM of IKK2 CA/CA mice. Consistent with the premature depletion of the HSC pool, IKK2 CA/CA HSCs exhibit a hyperproliferative phenotype and have compromised quiescence. Molecular analyses suggested that constitutive IKK2 signals induce an erythroid lineage-specific transcriptional program in HSCs. Among other genes that were differentially expressed in IKK2 CA/CA HSCs, the upregulation of *Klf1* and *Gata1* was very surprising, because they are believed to be erythroid lineage-restricted TFs (Siatecka and Bieker, 2011). Of note, Klf1 was the most highly expressed TF in IKK2 CA/CA HSCs. Another observation was that constitutive IKK2 signals caused a downregulation of *Gata2* and an upregulation of *Gata1* in HSCs. This inverse correlation between Gata2 and Gata1, possibly through the Gata switch (Suzuki et al., 2013), seems to be critical for the induction of erythroid differentiation pathways in HSPCs (Bresnick et al., 2010). Earlier studies have unequivocally demonstrated that Gata factors are essential for hematopoiesis; however, they need to be tightly controlled in HSPCs. In general, Gata2 is expressed in HSPCs and Gata1 is suppressed in HSPCs through Gata2-dependent mechanisms (Philipsen, 2013; Takai et al., 2013). The enforced expression of *Gata1* in HSCs leads to the loss of self-renewal capacity (Ferreira et al., 2007). Thus, the genetic changes observed in IKK2 CA/CA HSCs can be explained at least in part by the deregulated control of Gata1 and Gata2 expression. NF-κB has been shown to directly regulate the expression of Gata family members (Corn et al., 2005), and our *in silico* analysis identified the presence of putative NF-κB binding sites in the regulatory regions of *Gata1*. Based on these studies, it can be postulated that the constitutive activation of NF-κB results in augmented binding to *Gata1* and activates its expression in IKK2 CA/CA HSCs.

One of the direct and immediate downstream targets of Gata1 is *Klf1* (Crossley et al., 1994). Klf1 expression and activity are tightly controlled in a temporal and differentiation stage-specific manner (Yien and Bieker, 2013). Klf1 plays a role in facilitating and/or stabilizing Gata1 occupancy in the erythroid genes, contributing to the generation of active chromatin structures such as histone acetylation and chromatin looping (Kang et al., 2015). Gata1, stem cell leukemia (SCL), and Klf1 form an erythroid core transcriptional network by co-occupying >300 genes (Wontakal et al., 2012). The present study documented a defective regulatory circuit of Klf1 and identified a key functional consequence of elevated Klf1 expression in HSCs. In particular, our data identified a previously unappreciated role for Klf1 in the suppression of TPO signals and of *c-Mpl* expression in IKK2 CA/CA HSPCs. Signals mediated by TPO and its receptor c-Mpl are vital for the maintenance and quiescence of HSCs in the BM niche (Qian et al., 2007; Yoshihara et al., 2007) and for the

establishment of definitive hematopoiesis (Petit-Cocault et al., 2007). Loss of TPO signaling has been associated with BM failure (de Graaf and Metcalf, 2011).

Earlier studies demonstrated a dominant role for non-canonical NF-κB signals in both the intrinsic and extrinsic control of hematopoiesis (González-Murillo et al., 2015; Weih et al., 1995; Xiu et al., 2017; Zhao et al., 2012). While these studies underlined the importance of non-canonical NF-κB signaling, functions of the canonical arm of the NF-κB pathway need to be identified. Especially in light of the fact that canonical and non-canonical pathways of NF-κB are completely different and are activated by distinct upstream stimuli, governed by different components, and involved in the activation of specific transcriptional targets, conclusions and findings obtained from the studies involving non-canonical NF-κB pathway may not be attributed to the roles of canonical NF-κB signals, particularly in HSCs. Moreover, the precise downstream molecular consequences of increased NF-κB signals (both canonical and non-canonical) in HSCs have not been identified to date. A combined loss of p65 and c-Rel, key subunits of the canonical NF-κB pathway, resulted in severe hematopoietic defects, including failure to promote the survival of myeloablated mice, reduction of spleen CFU progenitors, impaired erythropoiesis, and deregulated expansion of granulocytes (Grossmann et al., 1999). However, loss of p65 in HSCs resulted in altered hematopoiesis, including increased numbers of HSPCs, increased cycling of HSPCs, decreased frequencies of lineage-committed progenitors, augmented extramedullary hematopoiesis, impaired reconstitution abilities of HSPCs, upregulation of lineage-restricted genes, and downregulation of genes involved in HSC maintenance and homeostasis (Stein and Baldwin, 2013). Based on these studies, it can be speculated that canonical NF-κB signals positively regulate HSC maintenance and functions. However, the data of our studies suggest that constitutive activation of canonical NF-κB signals lead to a more severe HSC phenotype than the HSC phenotype due to the loss of functions of NF-κB. It is also surprising to observe some interesting parallels between the loss of functions and gain of functions of NF-κB in HSCs, as both conditions lead to (1) impaired HSC quiescence, (2) reduced HSC repopulation capacities, (3) increased lineage signature, and (4) reduced HSC signature. A more detailed study is needed to understand the common and distinct molecular mechanisms that are used by HSCs under conditions that lead to either loss or gain of NF-κB signals.

In essence, the phenotype of IKK2 CA/CA mice may be explained by a combination of deregulated expression of erythroid-specific TFs leading to the induction of an erythroid-specific transcription program; reduced HSC quiescence due to diminished TPO signals caused by the suppression of *c-Mpl* by Klf1; and elevated expression of inflammatory cytokines, possibly due to increased NF-κB binding to their regulatory regions. Even though our mechanistic studies provide possible explanations of how constitutively active IKK2 signals may affect the physiology of HSCs, at least in part, we believe that additional mechanisms may be involved in the phenotype of IKK2 CA/CA mice. In particular, there is a possibility that some of the upregulated targets in IKK2 CA/CA HSCs may be directly regulated by NF-κB and that IKK2 may be activating pathways that are outside the realm of NF-κB. More detailed investigations addressing all of these aspects should be carried out in the near future. Nevertheless, the present study establishes a compelling model through which exaggerated NF-κB activity affects the HSC pool and contributes to pathophysiology.

STAR★METHODS

CONTACT FOR REAGENT AND RESOURCE SHARING

Further information and requests for resources and reagents should be directed to and will be fulfilled by the Lead Contact, Chozha V. Rathinam M.Sc., Ph.D. (crathinam@ihv.umaryland.edu)

EXPERIMENTAL MODEL AND SUBJECT DETAILS

Mice—R26Stop^{FL}ikk2ca (B6(Cg)-Gt(ROSA)26Sortm4(Ikbkb)Rsky/J) mice, Vav-iCre (B6.Cg-Commd10$^{Tg(Vav1-icre,A2Kio}$/J) mice, IFNγ$^{-/-}$ mice and Mx-Cre (B6.Cg-Tg(Mx1-cre)1Cgn/J) mice were purchased from the Jackson Laboratory. A20^{HemKO} (Tnfaip3$^{flox/flox}$ mice crossed with Vav-iCre mice) mice were previously described (Nakagawa et al., 2015). Flt3$^{Cre/+}$ mice were generated and reported earlier (Benz et al., 2008; Boyer et al., 2011) CD45.1 congenic animals were purchased from the National Cancer Institute. The Institutional Animal Care and Use Committee of Columbia University and University of Maryland School of Medicine approved all mouse experiments.

METHOD DETAILS

Cell preparation—CA/CA mice were analyzed at 14 d after birth (P14), unless otherwise specified. RBCs were lysed with ammonium chloride (STEMCELL Technologies). Trypan blue (Amresco)-negative cells were counted as live cells.

Flow cytometry—Cells were analyzed by flow cytometry with FACS Fortessa or LSR II (BD) and FACSDiva software (BD Biosciences) or FlowJo software (Tree Star). In all the FACS plots, indicated are the percentages (%) of the gated fraction.

Phosflow studies—To detect phosphorylation of STAT5 and ERK by flow cytometry, cells were either stimulated with TPO or SCF or IL3 or unstimulated for 30 minutes. Cells were first fixed, permeabilized using a commercially available phosflow kit (BD Pharmigen) and stained with either pSTAT5-PE and pERK-PE antibodies (BD biosciences) or total STAT5 primary antibodies (Cell Signaling) and anti-Rabbit PE secondary antibodies (Cell Signaling) according to the manufacturer's instructions.

BMT experiments—1×10^6 of bone marrow cells were injected into lethally irradiated (10 Gy) either congenic (CD45.1$^+$) WT recipient mice or control and IKK2$^{F/F}$ MX1$^{cre/+}$ (CD45.2+). For competitive-repopulation experiments, 4×10^5, 1.2×10^6, or 1×10^6 of BM cells from either control and CA/CA mice or control and IKK2$^{F/F}$ MX1$^{cre/+}$ mice were mixed with 4×10^5, 4×10^5, or 2×10^5 of WT (CD45.1$^+$) BM cells (to obtain a ratio of 1:1, 3:1, or 5:1, respectively) and were injected into lethally irradiated congenic WT (CD45.1$^+$) recipient mice.

Apoptosis assay—Apoptotic cells were detected by Annexin V PE Apoptosis Detection Kit according to the manufacturer's instructions (BD Bioscience).

Cell proliferation experiments—For BrdU assays, pregnant mice (E17) were injected i.p. with 1 mg BrdU (BD). At 16 h after injection, mice were sacrificed and fetal liver cells were stained for BrdU, according to the BrdU Flow kit (BD) manufacturer's instructions, and detected by flow cytometry.

Cell cycle analysis—Cells were stained with surface markers and fixed and permeabilized with Cytofix/Cytoperm fixation/permeabilization solution kit (BD). These cells were stained with Ki-67 (B56;BD) for 30 min and subsequently stained with 20 µg/ml Hoechst 33342 for 5 min and analyzed by flow cytometry.

ChIP assay—ChIP assay was performed with Pierce Agarose ChIP Kit (Pierce) according to the manufacturer's instructions. In brief, either 1×10^7 of bone marrow cells or 5×10^6 Lineage negative BM cells were fixed and immunoprecipitated with anti-Klf1 antibody (ab2483; abcam) or goat IgG (Thermo Fisher Scientific). Immunoprecipitated DNA fragments were quantified by real-time PCR with the use of the following primers, which amplify the Mpl promoter region containing possible Klf1 binding sites; forward 5′-GACAGCCATATGCTCTTCCT-3′, reverse, 5′-GGTTCCTTGTCAGATACAGCC-3′. Fold enrichment was normalized to goat IgG-precipitated samples.

RNA extraction, PCR, and real-time PCR—Total RNA was isolated with an RNeasy Mini kit or RNeasy Micro kit (QIAGEN). cDNA was synthesized with Oligo(dT) primer and Maxima reverse transcription (Thermo Fisher Scientific). PCR was performed with T100 thermal cycler (Bio-Rad Laboratories) and TSG Taq (Lamda Biotech). Real-time PCR was performed in duplicates with a CFX-connect real-time PCR system (Bio-Rad Laboratories) and SsoAd- vanced SYBR Green Supermix (Bio-Rad Laboratories) according to the manufacturer's instructions. Relative expression was normalized to the expression levels of the internal control (housekeeping gene) Hprt.

Microarray—For transcriptional profiling studies, HSPCs (Flt3^{low} LSK cells) from either control or CA/CA mice (n = 3–5/ sorting) were sorted and total RNA was isolated using the QIAGEN RNAeasy micro kit according to the manufacturer's instruction (QIAGEN). RNA samples from 5 independent sorts of control or CA/CA mice were pooled, respectively, and taken for microarray studies. Gene Expression profiling was performed using Illumina's MouseWG-6 v2.0 Expression Bead Chip at the Yale Center for Genome Analysis. Normalized expression data were collapsed to gene symbols with max probes by Collapse Dataset module in Gene Pattern. These genes were pre ranked for log2 fold change and analyzed with Gene Set Enrichment Analysis (GSEA). Two hundred most upregulated genes or 200 most downregulated genes in CA/CA HSCs were analyzed in GO Enrichment analysis (Mi et al., 2017)

Retrovirus production—Cell culture and retroviral transduction were performed as previously described with minor modification (Rathinam et al., 2010). Mouse hematopoietic cells were cutlred in RPMI (Thermo Fisher Scientific) with 10% FBS, 1% PS, 10ng/ml rm-IL3, rm-IL6, rm-TPO, rm-Flt3L and rm-SCF (PEPROTECH). For viral transduction, Cells were centrifused at 30 degree for 90 minutes at 2000 rpm with polybrene (8ug /ml). Plat-E packaging cells (Cell Bio labs) were used for retrovirus production. For making retrovirus

plasmid PGFP-RV-mKlf1, mouse Klf1 cDNA was cloned from pMXs-ms-Klf1 (a gift from Shinya Yamanaka, Add gene plasmid #50785) (Nakagawa et al., 2008) into PGFP-RV.

Reporter assay—Mouse *c-Mpl* promoter region (−496 ~+19) containing possible Klf1 binding sites was amplified from B6 wild-type mouse genome, and cloned into PGL3-basic (Promega). HEK293T cells were transfected with reporter (PGL3-basic-*c-Mpl*-promoter) and expression plasmid (PGFP-RV-mKlf1) using Lipofectamine 2000 (Thermo Fisher) according to the manufacturer's instructions. As a control of transfection efficiency, a plasmid expressing Renilla-luciferase was cotransfected. The cells were harvested 48 hours after transfection and assayed for luciferase activity using Dual-Luciferase reporter assay system (Promega) and MONOlight 3010 (BD).

QUANTIFICATION AND STATISTICAL ANALYSIS

Data represent mean and s.e.m. Two-tailed Student's t tests were used to assess statistical significance (*$p < 0.05$, **$p < 0.01$, *** < 0.001). For survival curve analysis, log rank test was used to assess statistical significance (*$p < 0.05$, **$p < 0.01$, *** < 0.001).

DATA AND SOFTWARE AVAILABILITY

The accession number for the microarray analysis of HSPCs from control or CA/CA mice is GEO: GSE121195.

Supplementary Material

Refer to Web version on PubMed Central for supplementary material.

ACKNOWLEDGMENTS

REFERENCES

Almarza E, Segovia JC, Guenechea G, Gómez SG, Ramírez A, and Bueren JA (2004). Regulatory elements of the vav gene drive transgene expression in hematopoietic stem cells from adult mice. Exp. Hematol 32, 360–364. [PubMed: 15050746]

Baldridge MT, King KY, Boles NC, Weksberg DC, and Goodell MA (2010). Quiescent haematopoietic stem cells are activated by IFN-gamma in response to chronic infection. Nature 465, 793–797. [PubMed: 20535209]

Benz C, Martins VC, Radtke F, and Bleul CC (2008). The stream of precursors that colonizes the thymus proceeds selectively through the early T lineage precursor stage of T cell development. J. Exp. Med 205, 1187–1199. [PubMed: 18458114]

Boyer SW, Schroeder AV, Smith-Berdan S, and Forsberg EC (2011). All hematopoietic cells develop from hematopoietic stem cells through Flk2/Flt3-positive progenitor cells. Cell Stem Cell 9, 64–73. [PubMed: 21726834]

Bresnick EH, Lee HY, Fujiwara T, Johnson KD, and Keles S (2010). GATA switches as developmental drivers. J. Biol. Chem 285, 31087–31093. [PubMed: 20670937]

Brown K, Gerstberger S, Carlson L, Franzoso G, and Siebenlist U (1995). Control of I kappa B-alpha proteolysis by site-specific, signal-induced phosphorylation. Science 267, 1485–1488. [PubMed: 7878466]

Cheshier SH, Morrison SJ, Liao X, and Weissman IL (1999). In vivo proliferation and cell cycle kinetics of long-term self-renewing hematopoietic stem cells. Proc. Natl. Acad. Sci. USA 96, 3120–3125. [PubMed: 10077647]

Cheung TH, and Rando TA (2013). Molecular regulation of stem cell quiescence. Nat. Rev. Mol. Cell Biol 14, 329–340. [PubMed: 23698583]

Corn RA, Hunter C, Liou HC, Siebenlist U, and Boothby MR (2005). Opposing roles for RelB and Bcl-3 in regulation of T-box expressed in T cells, GATA-3, and Th effector differentiation. J. Immunol 175, 2102–2110. [PubMed: 16081776]

Crossley M, Tsang AP, Bieker JJ, and Orkin SH (1994). Regulation of the erythroid Kruppel-like factor (EKLF) gene promoter by the erythroid transcription factor GATA-1. J. Biol. Chem 269, 15440–15444. [PubMed: 8195185]

de Boer J, Williams A, Skavdis G, Harker N, Coles M, Tolaini M, Norton T, Williams K, Roderick K, Potocnik AJ, and Kioussis D (2003). Transgenic mice with hematopoietic and lymphoid specific expression of Cre. Eur. J. Immunol 33, 314–325. [PubMed: 12548562]

de Bruin AM, Voermans C, and Nolte MA (2014). Impact of interferon-γ on hematopoiesis. Blood 124, 2479–2486. [PubMed: 25185711]

de Graaf CA, and Metcalf D (2011). Thrombopoietin and hematopoietic stem cells. Cell Cycle 10, 1582–1589. [PubMed: 21478671]

Essers MA, Offner S, Blanco-Bose WE, Waibler Z, Kalinke U, Duchosal MA, and Trumpp A (2009). IFNalpha activates dormant haematopoietic stem cells in vivo. Nature 458, 904–908. [PubMed: 19212321]

Ferreira R, Wai A, Shimizu R, Gillemans N, Rottier R, von Lindern M, Ohneda K, Grosveld F, Yamamoto M, and Philipsen S (2007). Dynamic regulation of Gata factor levels is more important than their identity. Blood 109, 5481–5490. [PubMed: 17327407]

Forsberg EC, Passegué E, Prohaska SS, Wagers AJ, Koeva M, Stuart JM, and Weissman IL (2010). Molecular signatures of quiescent, mobilized and leukemia-initiating hematopoietic stem cells. PLoS One 5, e8785. [PubMed: 20098702]

Foudi A, Hochedlinger K, Van Buren D, Schindler JW, Jaenisch R, Carey V, and Hock H (2009). Analysis of histone 2B-GFP retention reveals slowly cycling hematopoietic stem cells. Nat. Biotechnol 27, 84–90. [PubMed: 19060879]

Ghosh S, and Hayden MS (2008). New regulators of NF-kappaB in inflammation. Nat. Rev. Immunol 8, 837–848. [PubMed: 18927578]

González-Murillo Á, Fernández L, Baena S, Melen GJ, Sánchez R, Sánchez-Valdepeñas C, Segovia JC, Liou HC, Schmid R, Madero L, et al. (2015). The NFKB inducing kinase modulates hematopoiesis during stress. Stem Cells 33, 2825–2837. [PubMed: 26037670]

Grossmann M, Metcalf D, Merryfull J, Beg A, Baltimore D, and Gerondakis S (1999). The combined absence of the transcription factors Rel and RelA leads to multiple hemopoietic cell defects. Proc. Natl. Acad. Sci. USA 96, 11848–11853. [PubMed: 10518539]

Kang Y, Kim YW, Yun J, Shin J, and Kim A (2015). KLF1 stabilizes GATA-1 and TAL1 occupancy in the human β-globin locus. Biochim. Biophys. Acta 1849, 282–289. [PubMed: 25528728]

Karin M (2006). Nuclear factor-kappaB in cancer development and progression. Nature 441, 431–436. [PubMed: 16724054]

Kato Y, Iwama A, Tadokoro Y, Shimoda K, Minoguchi M, Akira S, Tanaka M, Miyajima A, Kitamura T, and Nakauchi H (2005). Selective activation of STAT5 unveils its role in stem cell self-renewal in normal and leukemic hematopoiesis. J. Exp. Med 202, 169–179. [PubMed: 15998795]

Kiel MJ, and Morrison SJ (2008). Uncertainty in the niches that maintain haematopoietic stem cells. Nat. Rev. Immunol 8, 290–301. [PubMed: 18323850]

King KY, Baldridge MT, Weksberg DC, Chambers SM, Lukov GL, Wu S, Boles NC, Jung SY, Qin J, Liu D, et al. (2011). Irgm1 protects hematopoietic stem cells by negative regulation of IFN signaling. Blood 118, 1525–1533. [PubMed: 21633090]

King B, Trimarchi T, Reavie L, Xu L, Mullenders J, Ntziachristos P, Aranda-Orgilles B, Perez-Garcia A, Shi J, Vakoc C, et al. (2013). The ubiquitin ligase FBXW7 modulates leukemia-initiating cell activity by regulating MYC stability. Cell 153, 1552–1566. [PubMed: 23791182]

Kondo M, Wagers AJ, Manz MG, Prohaska SS, Scherer DC, Beilhack GF, Shizuru JA, and Weissman IL (2003). Biology of hematopoietic stem cells and progenitors: implications for clinical application. Annu. Rev. Immunol 21, 759–806. [PubMed: 12615892]

Lienenklaus S, Walisko R, te Boekhorst A, May T, Samuelsson C, Michiels T, and Weiss S (2008). PCR-based simultaneous analysis of the interferon-alpha family reveals distinct kinetics for early interferons. J. Interferon Cytokine Res 28, 653–660. [PubMed: 18844580]

Matsumoto A, Takeishi S, Kanie T, Susaki E, Onoyama I, Tateishi Y, Nakayama K, and Nakayama KI (2011). p57 is required for quiescence and maintenance of adult hematopoietic stem cells. Cell Stem Cell 9, 262–271. [PubMed: 21885021]

Mercurio F, Zhu H, Murray BW, Shevchenko A, Bennett BL, Li J, Young DB, Barbosa M, Mann M, Manning A, and Rao A (1997). IKK-1 and IKK-2: cytokine-activated IkappaB kinases essential for NF-kappaB activation. Science 278, 860–866. [PubMed: 9346484]

Mi H, Huang X, Muruganujan A, Tang H, Mills C, Kang D, and Thomas PD (2017). PANTHER version 11: expanded annotation data from Gene Ontology and Reactome pathways, and data analysis tool enhancements. Nucleic Acids Res 45 (D1), D183–D189. [PubMed: 27899595]

Morrison SJ, and Weissman IL (1994). The long-term repopulating subset of hematopoietic stem cells is deterministic and isolatable by phenotype. Immunity 1, 661–673. [PubMed: 7541305]

Nakagawa M, Koyanagi M, Tanabe K, Takahashi K, Ichisaka T, Aoi T, Okita K, Mochiduki Y, Takizawa N, and Yamanaka S (2008). Generation of induced pluripotent stem cells without Myc from mouse and human fibroblasts. Nat. Biotechnol 26, 101–106. [PubMed: 18059259]

Nakagawa MM, Thummar K, Mandelbaum J, Pasqualucci L, and Rathinam CV (2015). Lack of the ubiquitin-editing enzyme A20 results in loss of hematopoietic stem cell quiescence. J. Exp. Med 212, 203–216. [PubMed: 25624445]

Orford KW, and Scadden DT (2008). Deconstructing stem cell self-renewal: genetic insights into cell-cycle regulation. Nat. Rev. Genet 9, 115–128. [PubMed: 18202695]

Ouyang W, Ranganath SH, Weindel K, Bhattacharya D, Murphy TL, Sha WC, and Murphy KM (1998). Inhibition of Th1 development mediated by GATA-3 through an IL-4-independent mechanism. Immunity 9, 745–755. [PubMed: 9846495]

Passegué E, Wagers AJ, Giuriato S, Anderson WC, and Weissman IL (2005). Global analysis of proliferation and cell cycle gene expression in the regulation of hematopoietic stem and progenitor cell fates. J. Exp. Med 202, 1599–1611. [PubMed: 16330818]

Petit-Cocault L, Volle-Challier C, Fleury M, Péault B, and Souyri M (2007). Dual role of Mpl receptor during the establishment of definitive hematopoiesis. Development 134, 3031–3040. [PubMed: 17634189]

Philipsen S (2013). A new twist to the GATA switch. Blood 122, 3391–3392. [PubMed: 24235125]

Pietras EM, Warr MR, and Passegué E (2011). Cell cycle regulation in hematopoietic stem cells. J. Cell Biol 195, 709–720. [PubMed: 22123859]

Qian H, Buza-Vidas N, Hyland CD, Jensen CT, Antonchuk J, Månsson R, Thoren LA, Ekblom M, Alexander WS, and Jacobsen SE (2007). Critical role of thrombopoietin in maintaining adult quiescent hematopoietic stem cells. Cell Stem Cell 1, 671–684. [PubMed: 18371408]

Rathinam C, Thien CB, Langdon WY, Gu H, and Flavell RA (2008). The E3 ubiquitin ligase c-Cbl restricts development and functions of hematopoietic stem cells. Genes Dev 22, 992–997. [PubMed: 18413713]

Rathinam C, Thien CB, Flavell RA, and Langdon WY (2010). Myeloid leukemia development in c-Cbl RING finger mutant mice is dependent on FLT3 signaling. Cancer Cell 18, 341–352. [PubMed: 20951944]

Rathinam C, Matesic LE, and Flavell RA (2011). The E3 ligase Itch is a negative regulator of the homeostasis and function of hematopoietic stem cells. Nat. Immunol 12, 399–407. [PubMed: 21478879]

Rothwarf DM, Zandi E, Natoli G, and Karin M (1998). IKK-gamma is an essential regulatory subunit of the IkappaB kinase complex. Nature 395, 297–300. [PubMed: 9751060]

Sasaki Y, Derudder E, Hobeika E, Pelanda R, Reth M, Rajewsky K, and Schmidt-Supprian M (2006). Canonical NF-kappaB activity, dispensable for B cell development, replaces BAFF-receptor

signals and promotes B cell proliferation upon activation. Immunity 24, 729–739. [PubMed: 16782029]

Seita J, Sahoo D, Rossi DJ, Bhattacharya D, Serwold T, Inlay MA, Ehrlich LI, Fathman JW, Dill DL, and Weissman IL (2012). Gene Expression Commons: an open platform for absolute gene expression profiling. PLoS One 7, e40321. [PubMed: 22815738]

Siatecka M, and Bieker JJ (2011). The multifunctional role of EKLF/KLF1 during erythropoiesis. Blood 118, 2044–2054. [PubMed: 21613252]

Starck J, Cohet N, Gonnet C, Sarrazin S, Doubeikovskaia Z, Doubeikovski A, Verger A, Duterque-Coquillaud M, and Morle F (2003). Functional cross-antagonism between transcription factors FLI-1 and EKLF. Mol. Cell. Biol 23, 1390–1402. [PubMed: 12556498]

Stein SJ, and Baldwin AS (2013). Deletion of the NF-κB subunit p65/RelA in the hematopoietic compartment leads to defects in hematopoietic stem cell function. Blood 121, 5015–5024. [PubMed: 23670180]

Subramanian A, Tamayo P, Mootha VK, Mukherjee S, Ebert BL, Gillette MA, Paulovich A, Pomeroy SL, Golub TR, Lander ES, and Mesirov JP (2005). Gene set enrichment analysis: a knowledge-based approach for interpreting genome-wide expression profiles. Proc. Natl. Acad. Sci. USA 102, 15545–15550. [PubMed: 16199517]

Suzuki M, Kobayashi-Osaki M, Tsutsumi S, Pan X, Ohmori S, Takai J, Moriguchi T, Ohneda O, Ohneda K, Shimizu R, et al. (2013). GATA factor switching from GATA2 to GATA1 contributes to erythroid differentiation. Genes Cells 18, 921–933. [PubMed: 23911012]

Takai J, Moriguchi T, Suzuki M, Yu L, Ohneda K, and Yamamoto M (2013). The Gata1 5′ region harbors distinct cis-regulatory modules that direct gene activation in erythroid cells and gene inactivation in HSCs. Blood 122, 3450–3460. [PubMed: 24021675]

Tesio M, and Trumpp A (2011). Breaking the cell cycle of HSCs by p57 and friends. Cell Stem Cell 9, 187–192. [PubMed: 21885016]

Trumpp A, Essers M, and Wilson A (2010). Awakening dormant haematopoietic stem cells. Nat. Rev. Immunol 10, 201–209. [PubMed: 20182459]

Vallabhapurapu S, and Karin M (2009). Regulation and function of NF-kappaB transcription factors in the immune system. Annu. Rev. Immunol 27, 693–733. [PubMed: 19302050]

van der Wath RC, Wilson A, Laurenti E, Trumpp A, and Liò P (2009). Estimating dormant and active hematopoietic stem cell kinetics through extensive modeling of bromodeoxyuridine label-retaining cell dynamics. PLoS One 4, e6972. [PubMed: 19771180]

Venezia TA, Merchant AA, Ramos CA, Whitehouse NL, Young AS, Shaw CA, and Goodell MA (2004). Molecular signatures of proliferation and quiescence in hematopoietic stem cells. PLoS Biol 2, e301. [PubMed: 15459755]

Weih F, Carrasco D, Durham SK, Barton DS, Rizzo CA, Ryseck RP, Lira SA, and Bravo R (1995). Multiorgan inflammation and hematopoietic abnormalities in mice with a targeted disruption of RelB, a member of the NF-kappa B/Rel family. Cell 80, 331–340. [PubMed: 7834753]

Wilson A, and Trumpp A (2006). Bone-marrow haematopoietic-stem-cell niches. Nat. Rev. Immunol 6, 93–106. [PubMed: 16491134]

Wilson A, Laurenti E, Oser G, van der Wath RC, Blanco-Bose W, Jaworski M, Offner S, Dunant CF, Eshkind L, Bockamp E, et al. (2008). Hematopoietic stem cells reversibly switch from dormancy to self-renewal during homeostasis and repair. Cell 135, 1118–1129. [PubMed: 19062086]

Wontakal SN, Guo X, Smith C, MacCarthy T, Bresnick EH, Bergman A, Snyder MP, Weissman SM, Zheng D, and Skoultchi AI (2012). A core erythroid transcriptional network is repressed by a master regulator of myelo-lymphoid differentiation. Proc. Natl. Acad. Sci. USA 109, 3832–3837. [PubMed: 22357756]

Xiu Y, Xue WY, Lambertz A, Leidinger M, Gibson-Corley K, and Zhao C (2017). Constitutive activation of NIK Impairs the Self-Renewal of Hematopoietic Stem/Progenitor Cells and Induces Bone Marrow Failure. Stem Cells 35, 777–786. [PubMed: 27733012]

Yamaoka S, Courtois G, Bessia C, Whiteside ST, Weil R, Agou F, Kirk HE, Kay RJ, and Israël A (1998). Complementation cloning of NEMO, a component of the IkappaB kinase complex essential for NF-kappaB activation. Cell 93, 1231–1240. [PubMed: 9657155]

Yamazaki S, and Nakauchi H (2009). Insights into signaling and function of hematopoietic stem cells at the single-cell level. Curr. Opin. Hematol 16, 255–258. [PubMed: 19465850]

Yien YY, and Bieker JJ (2013). EKLF/KLF1, a tissue-restricted integrator of transcriptional control, chromatin remodeling, and lineage determination. Mol. Cell. Biol 33, 4–13. [PubMed: 23090966]

Yoshihara H, Arai F, Hosokawa K, Hagiwara T, Takubo K, Nakamura Y, Gomei Y, Iwasaki H, Matsuoka S, Miyamoto K, et al. (2007). Thrombopoietin/MPL signaling regulates hematopoietic stem cell quiescence and interaction with the osteoblastic niche. Cell Stem Cell 1, 685–697. [PubMed: 18371409]

Zandi E, Rothwarf DM, Delhase M, Hayakawa M, and Karin M (1997). The IkappaB kinase complex (IKK) contains two kinase subunits, IKKalpha and IKKbeta, necessary for IkappaB phosphorylation and NF-kappaB activation. Cell 91, 243–252. [PubMed: 9346241]

Zhao C, Xiu Y, Ashton J, Xing L, Morita Y, Jordan CT, and Boyce BF (2012). Noncanonical NF-κB signaling regulates hematopoietic stem cell self-renewal and microenvironment interactions. Stem Cells 30, 709–718. [PubMed: 22290873]

Zou P, Yoshihara H, Hosokawa K, Tai I, Shinmyozu K, Tsukahara F, Maru Y, Nakayama K, Nakayama KI, and Suda T (2011). p57(Kip2) and p27(Kip1) cooperate to maintain hematopoietic stem cell quiescence through interactions with Hsc70. Cell Stem Cell 9, 247–261. [PubMed: 21885020]

Highlights

- Constitutive activation of IKK2 causes pancytopenia and bone marrow failure

- Deregulated IKK2 signals cause loss of quiescence and depletion of HSC pool

- Augmented IKK2 induces erythroid transcription program in HSCs

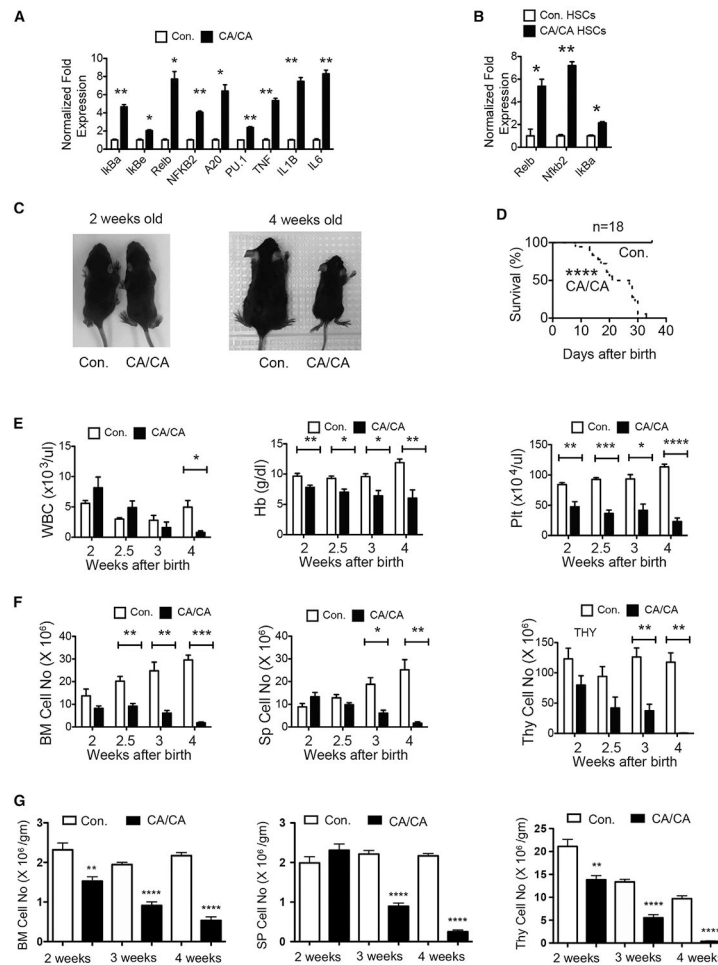- Increased IKK2 activation perturbs TPO signaling due to suppression of c-Mpl by Klf-1

Figure 1. Deregulated Canonical NF-κB Activation in HSCs Leads to Pancytopenia and Progressive BM Failure

(A) NF-κB target gene expressions in total BM of 14-day-old CA/CA and control mice. Representative data from two independent experiments.

(B) NF-κB target gene expressions in HSCs (CD150$^+$ LSK cells) of 14-day-old CA/CA and control mice. Representative data from two independent experiments.

(C) Representative pictures of CA/CA and control mice at 2 weeks old (left) and 4 weeks old (right).

(D) Kaplan-Meier survival curve analysis of CA/CA and control mice (n = 18). Significance (****p < 0.0001) was assessed using the log-rank test.

(E) Complete blood count (CBC) analysis of CA/CA and control mice (n = 3–6 at each time point). Hb, hemoglobin; Plt, platelet.

(F) Cell number of hematopoietic organs from CA/CA and control mice (n = 3–6 at each time point). Sp, spleen; Thy, thymus.

(G) Normalized (cell number per gram body weight) cell counts of hematopoietic organs from CA/CA and control mice (n = 8 at each time point).

All of the data represent means ± SEMs. Two-tailed Student's t tests were used to assess statistical significance (*p < 0.05, **p < 0.01, ***p < 0.001, ****p < 0.0001).
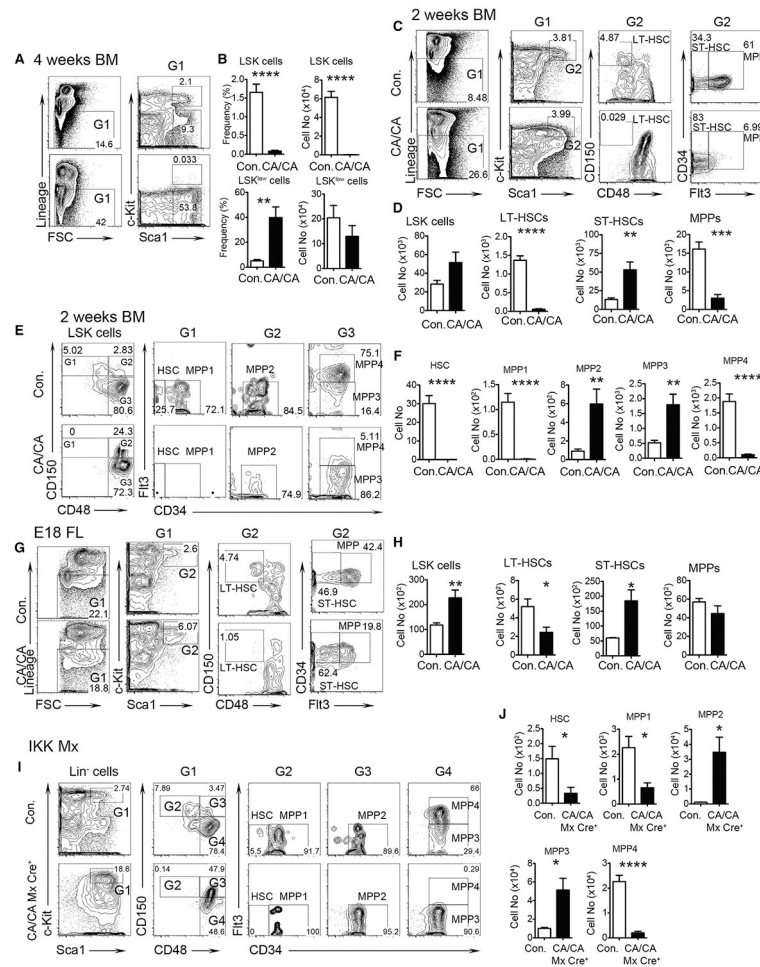
Figure 2. Constitutive Activation of IKK2 Results in a Complete Loss of HSPC Pool

(A) Fluorescence-activated cell sorting (FACS) plots of LSK cells and LSK^{low} cells from the BM (two femurs and two tibias) of 4-week-old CA/CA and control mice. Data are representative of three independent experiments.

(B) Absolute numbers of LSK cells and LSK^{low} cells from the BM (two femurs and two tibias) of 4-week-old CA/CA (n = 3, duplicate) and control (n = 3, duplicate) mice.

(C) FACS plots of LSK cells, LT-HSCs, ST-HSCs, and MPPs from the BM (two femurs and two tibias) of 2-week-old CA/CA and control mice. Data are representative of four independent experiments.

(D) Absolute numbers of LSK cells, LT-HSCs, ST-HSCs, and MPPs from the BM (two femurs and two tibias) of 2-week-old CA/CA (n = 4) and control (n = 5) mice.

(E) FACS plots of quiescent HSCs and MPP subsets in the BM of 2-week-old CA/CA and control mice. Data are representative of six independent experiments.

(F) Absolute numbers of quiescent HSCs and MPP subsets in the BM (two femurs and two tibias) of 2-week-old CA/CA (n = 6) and control (n = 7) mice.

(G) FACS plots of LSK cells, LT-HSCs, ST-HSCs, and MPPs from the liver of embryonic day 18 (E18) CA/CA and control fetus. Data are representative of three independent experiments.

(H) Absolute numbers of LSK cells, LT-HSCs, ST-HSCs, and MPPs from the fetal livers of E18 CA/CA (n = 3) and control (n = 3) mice.

(I and J) FACS plots (I) and absolute numbers (J) of quiescent HSCs and MPP subsets in the BM (two femurs and two tibias) of 6-week-old CA/CA Mx Cre$^+$ and control mice (2 weeks after poly I: pol C [PI:PC] injection) (n = 5). GFP$^+$ cells were pre-gated for CA/CA Mx Cre$^+$ mice.

All of the data represent means ± SEMs. Two-tailed Student's t tests were used to assess statistical significance (*p < 0.05, **p < 0.01, ***p < 0.001, ****p < 0.0001).
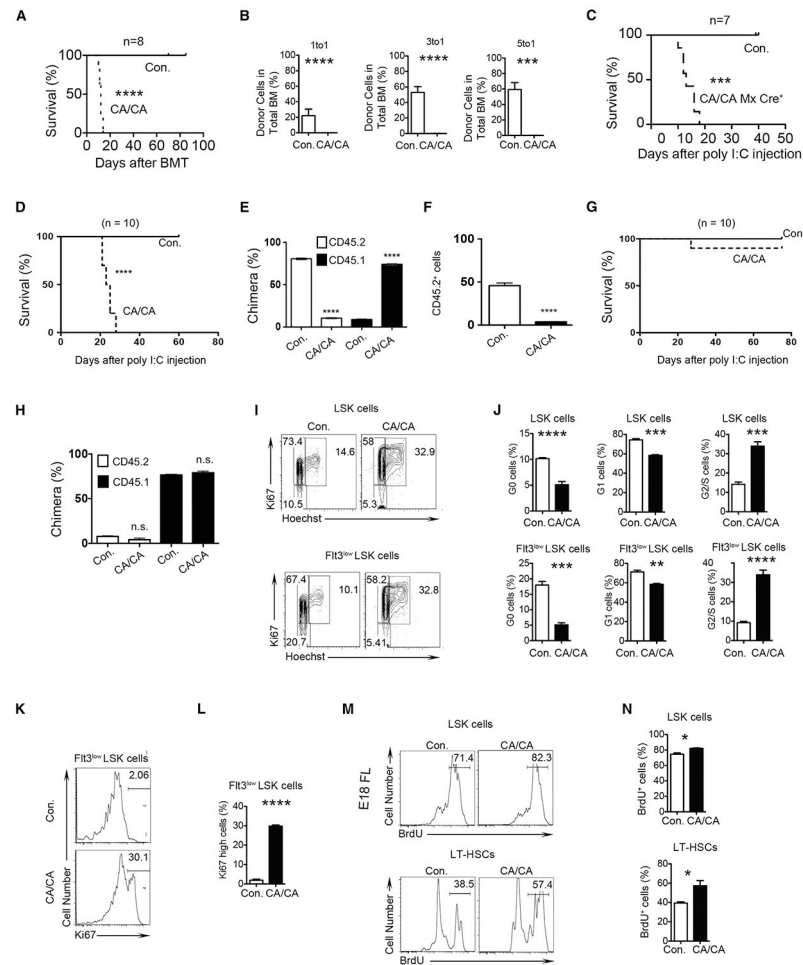
Figure 3. Augmented NF-κB Signals Affect HSC Functions and Lead to Loss of HSC Quiescence

(A) Kaplan-Meier survival curve analysis of WT recipients (CD45.1$^+$) that received the BM of either CA/CA or control mice (CD45.2$^+$) following lethal (10 Gy) irradiation. Each group represents data from a pool of eight animals. Significance (p < 0.0001) was assessed using the log-rank test.

(B) Frequencies of donor (CD45.2$^+$) hematopoiesis in the peripheral blood of WT recipients, 4 weeks after transplantation. Recipients received mixed chimera containing donor (CD45.2$^+$) BM cells (from either CA/CA or control mice) and WT competitor (CD45.1$^+$) BM cells at a ratio of 1:1 (left), 3:1 (middle), and 5:1 (right), respectively. Data are a pool of two independent experiments with two to eight mice per group.

(C) Kaplan-Meier survival curve analysis of WT recipients (CD45.1$^+$) that received the BM of either CA/CA Mx Cre$^+$ or control mice (CD45.2$^+$) following lethal (10 Gy) irradiation (n = 7). Significance (p = 0.0002) was assessed using the log-rank test.

(D) Kaplan-Meier survival curve analysis. WT recipients (CD45.1$^+$) were lethally irradiated and injected with the BM of either CA/CA Mx Cre$^+$ or control mice (CD45.2$^+$). Four weeks after BMT, recipients were injected with polyI:C and survival was recorded after the last dose of polyI:C (n = 10). Significance (p = 0.0001) was assessed using the log-rank test.

(E) Frequencies of donor (CD45.2$^+$)- and recipient (CD45.1$^+$)-derived hematopoiesis in the peripheral blood of WT recipients, 2 weeks after the last dose of polyI:C injection. Lethally

irradiated WT (CD45.1$^+$) recipients were injected with total BM of either control or CA/CA Mx Cre$^+$ 4 weeks before polyI:C injection (n = 10).

(F) Mixed BM chimera experiment. Frequencies of donor (control and CA/CA Mx Cre$^+$; CD45.2$^+$)-derived hematopoiesis in the peripheral blood of WT recipients, 4 weeks after the last dose of polyI:C injection. Lethally irradiated WT (CD45.1$^+$) recipients were injected with mixed BM of either control + WT(CD45.1$^+$) or CA/CA Mx Cre$^+$ + WT (CD45.1$^+$) 4 weeks before polyI:C injection (n = 10).

(G) Kaplan-Meier survival curve analysis. Control or CA/CA Mx Cre$^+$ recipients (CD45.2$^+$) were lethally irradiated and injected with BM of WT mice (CD45.1$^+$). Four weeks after BMT, recipients were injected with polyI:C, and survival was recorded after the last dose of polyI:C (n = 10). Significance (p = 0.0001) was assessed using the log-rank test.

(H) Frequencies of donor (CD45.1$^+$)- and recipient (CD45.2$^+$)-derived hematopoiesis in the peripheral blood of WT recipients, 8 weeks after the last dose of polyI:C injection. Lethally irradiated WT (CD45.1$^+$) recipients were injected with total BM of either control or CA/CA Mx Cre$^+$ 4 weeks before polyI:C injection (n = 10). (I and J) Representative FACS plots (I) and bar graphs (J) indicating the frequencies of LSK cells (top) and Flt3^{low} LSK cells (bottom) in G0 (Ki-67$^-$ and Hoechst$^-$), G1 (Ki-67$^+$ and Hoechst$^-$) and G2/S (Ki-67$^+$ and Hoechst$^+$) phase of the cell cycle in the BM of 2-week-old CA/CA (n = 3) and control (n = 5) mice.

(K and L) Representative FACS plots (K) and bar graphs (L) indicating the frequencies of cells with high Ki67 expression in Flt3^{low} LSK cells from the BM of 2-week-old CA/CA (n = 3) and control (n = 5) mice.

(M and N) Representative FACS plots (M) and bar graphs (N) indicating the frequencies of BrdU$^+$ cells in LSK cells and LT-HSCs in the fetal livers of E18 CA/CA and control mice, following 16-hr pulse with BrdU (n = 3).

All of the data represent means ± SEMs. Two-tailed Student's t tests were used to assess statistical significance (*p < 0.05, **p < 0.01, ***p < 0.001, ****p< 0.0001, ns, not significant).
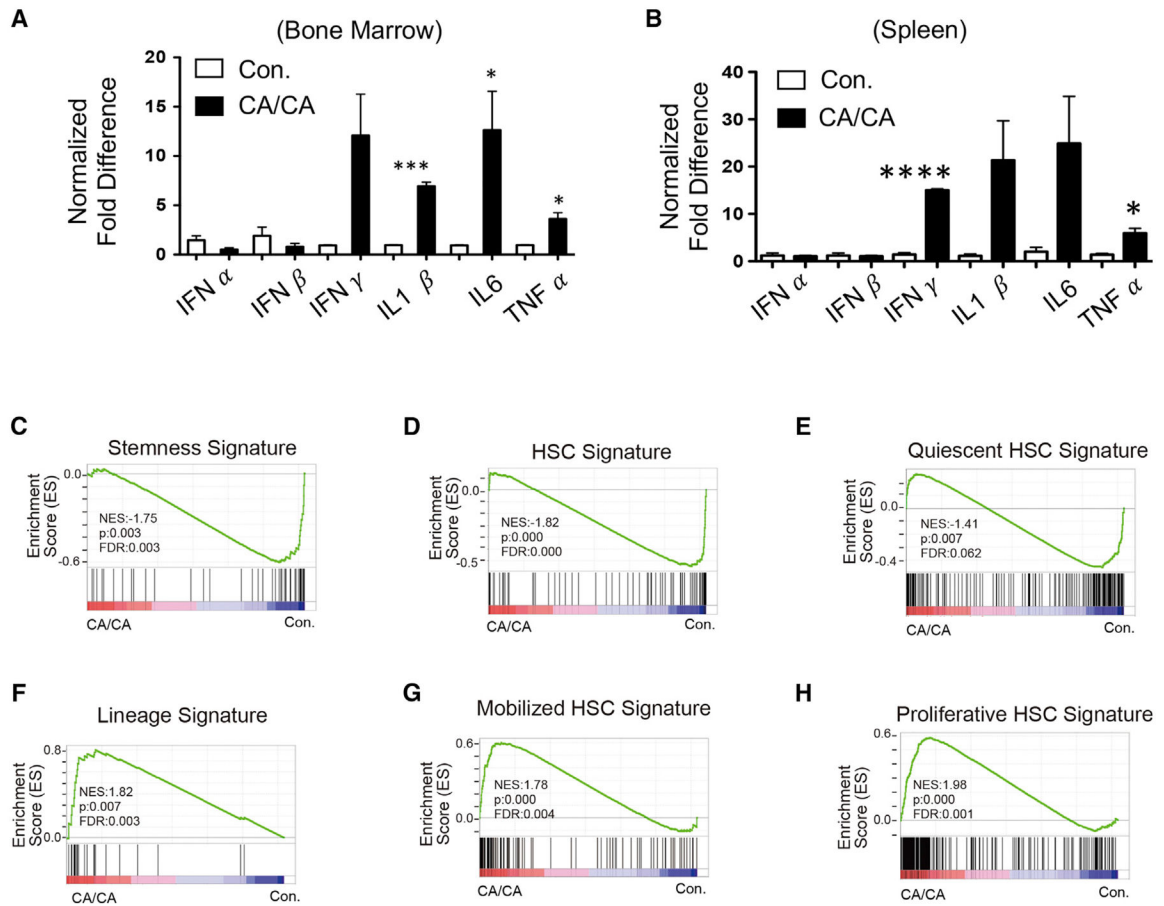
Figure 4. Deregulated Expression of Inflammatory Cytokines and Molecular Signatures of HSCs in CA/CA Mice

(A and B) Real-time PCR data documenting the increased expression levels of inflammatory cytokines in the BM (A) and spleen (B) of IKK2 mutant mice. Shown are cumulative data of independent animals (n = 3) of each group (control and CA/CA).

(C–H) Gene set enrichment analysis (GSEA) of microarray data from CA/CA versus control HSCs with the following gene sets: (C) stem cell genes, which are commonly upregulated in HSCs, muscle stem cells (MuSCs), and hair follicle stem cells (HFSCs); (D) genes enriched in normal, steady-state BM HSCs from WT mice compared to multipotent progenitors (MPPs), leukemic stem cells (LSCs), and mobilized HSCs; (E) genes enriched in quiescent HSCs, which are commonly upregulated in adult HSCs (versus fetal liver HSCs) and 0, 1, 10, and 30 days after 5-FU injection (versus 2, 3, and 6 days after 5-FU injection); (F) lineage-committed genes, which are commonly downregulated in HSCs, MuSCs, and HFSCs; (G) genes enriched in day +2 mobilized HSC by cyclophosphamide/GCSF compared to HSC at steady state; and (H) genes commonly upregulated in fetal liver HSCs (versus adult HSCs) and 2, 3, and 6 days after 5-FU injection (versus 0, 1, 10, and 30 days after 5-FU injection).

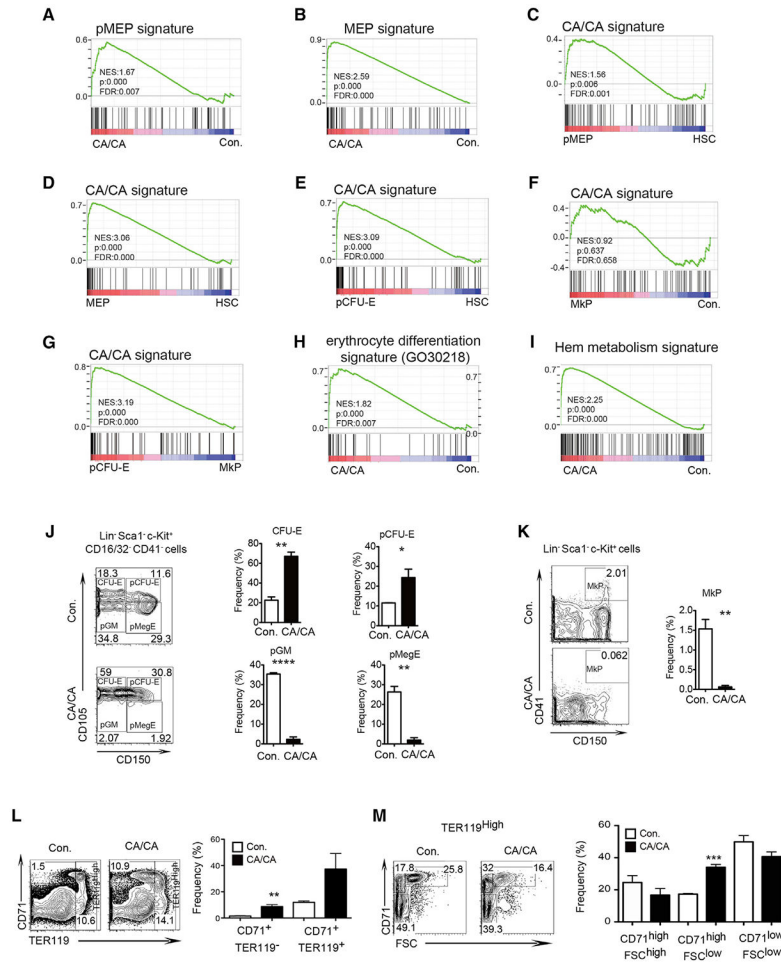$*p < 0.05$, $***p < 0.001$, $****p < 0.0001$.

Figure 5. Decontrolled IKK2 Activity Induces Erythroid Lineage-Specific Transcriptional Program in HSCs

(A and B) GSEA of microarray data from CA/CA versus control HSCs with the following gene sets: top 100 genes upregulated in pMEPs compared to HSCs (A) and top 100 genes upregulated in MEPs compared to HSCs (B).

(C–G) GSEA of microarray data from pMEPs (C), MEPs (D), pCFU-Es (E), and MkPs (F) versus HSCs, with the genes enriched in CA/CA HSCs compared to control HSCs. GSEA of microarray data from pCFU-Es versus MkPs, with the genes enriched in CA/CA HSCs compared to control HSCs (G).

(H and I) GSEA of microarray data from CA/CA versus control HSCs with the following gene sets: genes that are involved in erythroid differentiation (H) and genes that are involved in heme metabolism and erythroid differentiation (I).

(J and K) Representative FACS plots and bar graphs indicating frequencies of CFU-E, pCFU-E, pGM, and pMegE (J), and MkP (K) in the BM of CA/CA mice. (L and M) Representative FACS plots and bar graphs indicating frequencies of pro-erythrocytes (CD71$^+$Ter119$^-$), immature erythroblasts (TER119^{high}CD71^{high}FSC^{high}), less mature erythroblasts (TER119^{hgh}CD71^{high}FSC^{low}, and most mature erythroblasts (TER119^{high}CD71^{low}FSC^{low}) in the BM of CA/CA mice (n = 3). TER119^{high} cells from (L) were pre-gated and further distinguished based on CD71 expression and forward scatter (M).

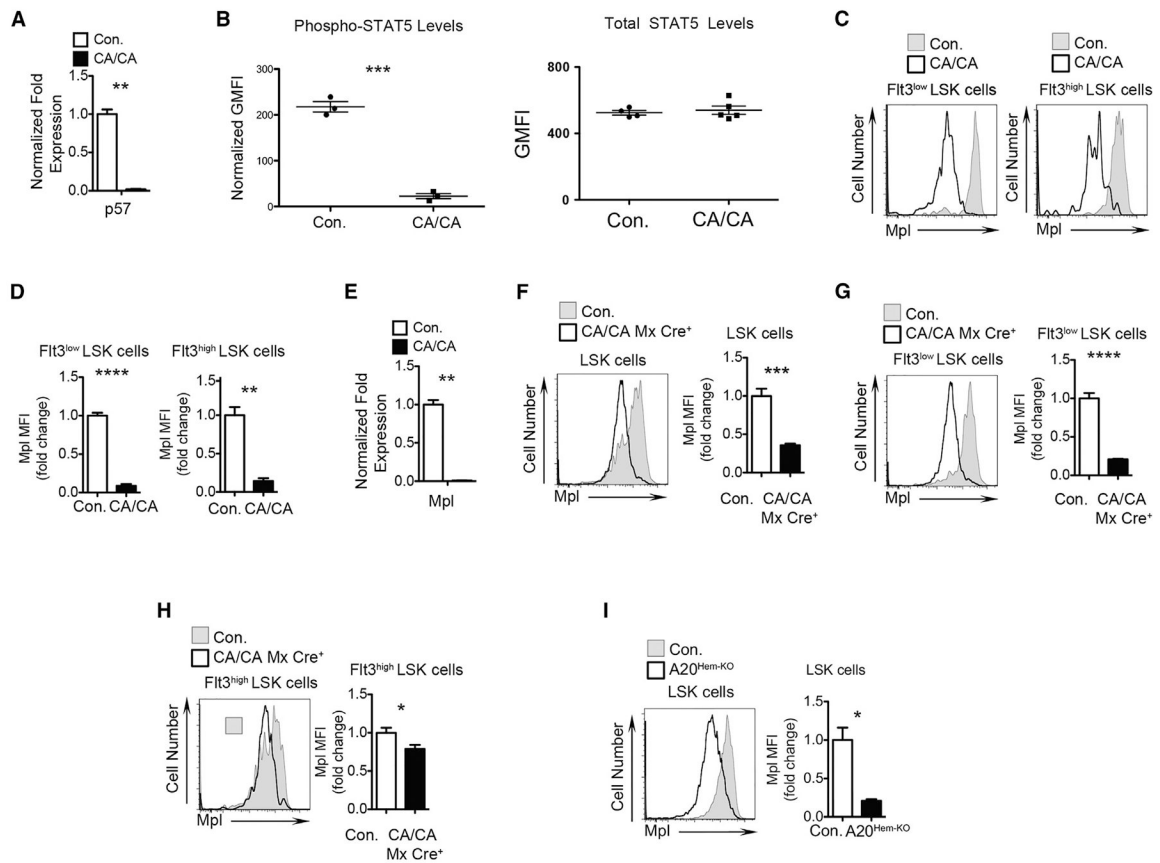*p < 0.05, ***p < 0.001, ****p < 0.0001.

Figure 6. Constitutive Activation of IKK2 Causes Cell-Intrinsic Suppression of c-Mpl in HSPCs

(A) Real-time PCR data for *Cdknlc (p57)* in Flt3^{low} LSK cells from the BM of 2-week-old CA/CA or control mice. Expression levels of target genes were normalized to hypoxanthine-guanine phosphoribosyltransferase (*Hprt*) levels. Data are representative of two independent experiments.

(B) Phosflow analysis indicating reduced levels of phospho-STAT5 and normal levels of total STAT5 in CA/CA LSK cells in response to TPO. Shown are the geometric mean fluorescence intensity (GMFI) of control and CA/CA cells after normalizing to the unstained cells of the respective groups (n = 3–5).

(C and D) Surface expression of c-Mpl in Flt3^{low} LSK cells (left) and Flt3^{hgh} LSK cells (right) from the BM of 2-week-old CA/CA or control mice. Representative FACS plots (C) and bar graphs of GMFI (D) (n = 3).

(E) Real-time PCR data for *c-Mpl* in Flt3^{low} LSK cells from the BM of 2-week-old CA/CA or control mice. Expression levels of target genes were normalized to *Hprt* levels. Data are representative of two independent experiments.

(F–H) Surface expression of c-Mpl in LSK cells (F), Flt3^{low} LSK cells (G), and Flt3^{high} LSK cells (H) from the BM of 6-week-old CA/CA Mx Cre^{+} and control mice (2 weeks after PI:PC injection). Representative FACS plots (left) and bar graphs of MFI (right) (n = 5).

(I) Surface expression of c-Mpl in LSK cells from the BM of 2-week-old A20^{Hem-KO} or control mice. Representative FACS plots (left) and bar graphs of MFI (right) (n = 2).

All of the data represent means ± SEMs. Two-tailed Student's t tests were used to assess statistical significance (*p < 0.05, **p < 0.01, ***p < 0.001, ****p < 0.0001).
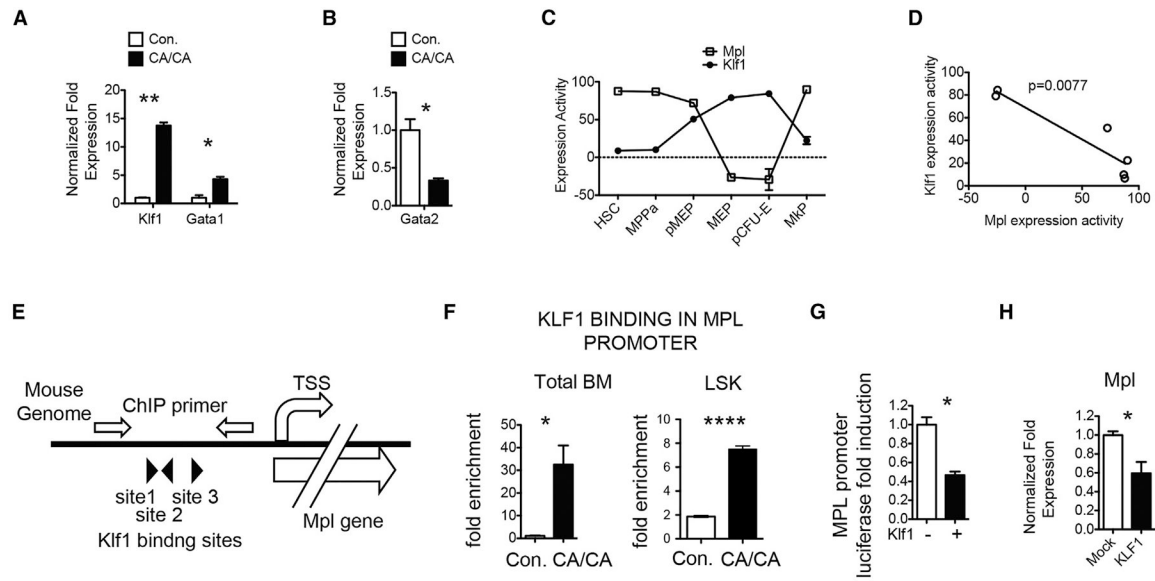
Figure 7. Klf1 Acts as a Transcriptional Repressor of *c-Mpl* in HSPCs

(A and B) Real-time PCR data for *Klf1* and *Gata1* (A), and Gata2 (B), in Flt3^{low} LSK cells from the BM of 2-week-old CA/CA or control mice. Expression levels of target genes were normalized to *Hprt* levels. Data are representative of two independent experiments.

(C and D) Expression activity (C) and correlation (D) of c-Mpl (1421461_at) and Klf1 (1418600_at) in WT mouse HSPCs. Probeset with a more dynamic range was chosen if the gene had more than one probeset. Two-tailed Pearson correlation test was performed.

(E) Diagrammatic representation of the *c-Mpl* gene, indicating the presence of Klf1 binding sites in its promoter.

(F) ChIP analysis of Klf1 binding to the *c-Mpl* promoter in the BM or Lin$^-$ cells of 2-week-old CA/CA or control mice. Shown are the real-time PCR data of Klf1 immunoprecipitates, which were normalized to immunoglobulin G (IgG) control immunoprecipitates. Data are representative of two independent experiments.

(G) *c-Mpl* promoter (−496 to 19) luciferase assay in 293T cells with and without the exogenous expression of Klf1. Data are representative of two independent experiments.

(H) Real-time PCR data for *c-Mpl* in GFP$^+$ cells from Mock and Klf1 transduced LSK cells. Expression levels of target genes were normalized to *Hprt* levels. Data are representative of two independent experiments.

All of the data represent means ± SEMs. Two-tailed Student's t tests were used to assess statistical significance (*p < 0.05, **p < 0.01, ****p < 0.0001).

KEY RESOURCES TABLE

REAGENT or RESOURCE	SOURCE	IDENTIFIER
Experimental Models: Organisms/Strains		
Mouse: R26Stop^FL-ikk2ca	The Jackson Laboratory	JAX:008242
Mouse: Vav-iCre	The Jackson Laboratory	JAX:008610
Mouse: IFNγ$^{-/-}$	The Jackson Laboratory	JAX:002287
Mouse: Mx-Cre	The Jackson Laboratory	JAX:003556
Mouse: Tnfaip3^flox/flox	Nakagawa et al., 2015	N/A
Mouse: Flt3^Cre/+ mice	Benz et al., 2008; Boyer et al., 2011	N/A
Mouse: CD45.1 congenic animals	National Cancer Institute	Charles River: 564
Antibodies for flow cytometry		
Rat anti-CD34 (clone RAM34)	BD Biosciences	#560238, #551387
Hamster anti-CD48 (HM48–1)	BD Biosciences	#747718
Rat anti-CD117(c-Kit) (2B8)	BD Biosciences	#560250
Rat anti-Flt3 (A2F10.1)	BD Biosciences	# 560718
Rat anti-Sca-1 (D7)	BD Biosciences	# 558162
Rat anti-B220 (RA3–6B2)	BD Biosciences	# 553086, # 561881
Rat anti-CD19 (1D3)	BD Biosciences	# 553784, # 561739
Hamster anti-CD3 (145–2C11)	BD Biosciences	# 553059, # 55277
Rat anti-CD4 (GK1.5)	BD Biosciences	# 563933, # 563933
Rat anti-CD8 (53–6.7)	BD Biosciences	# 553028,# 552877
Rat anti-CD11b (M1/70)	BD Biosciences	#553309,# 552850
Rat anti-Gr-1 (RB6–8C5)	BD Biosciences	# 553125,# 565033
anti-Ter119 (TER119)	BD Biosciences	# 553672,# 557853
Rat anti-CD71 (C2)	BD Biosciences	#561937
Mouse anti-CD45.1 (A20)	BD Biosciences	# 561872
Mouse anti-CD45.2 (104)	BD Biosciences	# 562895
Rat anti-CD150 (TC15–12F12.2)	Biolegend	#115910, #115929
Rat anti-CD41(MWReg30)	Biolegend	# 133916
Rat anti-CD105 (MJ7/18)	Biolegend	# 120408
Rat anti-CD16/32 (93)	Biolegend	#101308, #101303
Rat anti-Mpl (AMM2)	IBL	# 10403
PerCP-Cy5.54 Streptavidin	BD Biosciences	#551419
PE-Cy7 Streptavidin	BD Biosciences	#554063
Mouse anti-Ki-67 (B56)	BD Biosciences	# 561126
Rabbit anti-STAT5	Cell Signaling	#94205
Mouse anti-pSTAT5-PE	BD Biosciences	#562077
Mouse anti-pERK	BD Biosciences	# 560388
Anti-Rabbit IgG-PE	Cell Signaling	# 8885
Antibodies for ChIP		

REAGENT or RESOURCE	SOURCE	IDENTIFIER
anti-Klf1 antibody	anti-Klf1 antibody (ab2483; abcam)	anti-Klf1 antibody (ab2483; abcam)
Goat IgG Isotype Control antibody	Goat IgG Isotype Control antibody	Goat IgG Isotype Control antibody
Deposited Data		
Microarray data	This paper	GEO: GSE121195
Oligonucleotides		
ChIP primer forward for Mpl promoter region containing possible Klf1 binding sites 5′-GACAGCCATATGCTCTTCCT-3′,	This paper	N/A
ChIP primer reverse for Mpl promoter region containing possible Klf1 binding sites 5′-GGTTCCTTGTCAGATACAGCC-3′.	This paper	N/A
qPCR primer forward for Ikba:TCGCTCTTGTTGAAATGTGGG	This paper	N/A
qPCR primer reverse for Ikba:ATAGGGCAGCTCATCCTCTG	This paper	N/A
qPCR primer forward for Ikbe:GGACTCCACTTATGCCTCCT	This paper	N/A
qPCR primer reverse for Ikbe:CAGTGCTGTCTGGTAAAGGT	This paper	N/A
qPCR primer forward for Relb:TCTACGACAAGAAGTCCACCA	This paper	N/A
qPCR primer reverse for Relb:TTTGAACACAATGGCGATCTG	This paper	N/A
qPCR primer forward for Nfkb2:GACGAAGTTTATTTGCTCTGTG	This paper	N/A
qPCR primer reverse for Nfkb2:CTTCCTCCTTGTCTTCCACC	This paper	N/A
qPCR primer forward for A20:CAGAAGAAGCTCAACTGGTGTC	This paper	N/A
qPCR primer reverse for A20:ATTCCAGTTCCGAGTGTCGT	This paper	N/A
qPCR primer forward for Pu.1:GAAAGCCATAGCGATCACTACTG	This paper	N/A
qPCR primer reverse for Pu.1:GGGACAAGGTTTGATAAGGGA	This paper	N/A
qPCR primer forward for Tnf:TCTCAGCCTCTTCTCATTCCT	This paper	N/A
qPCR primer reverse for Tnf:ACTTGGTGGTTTGCTACGAC	This paper	N/A
qPCR primer forward for Il1b:TTTGACAGTGATGAGAATGACC	This paper	N/A
qPCR primer reverse for Il1b:AATGAGTGATACTGCCTGCC	This paper	N/A
qPCR primer forward for Il6:CTCTGCAAGAGACTTCCATCC	This paper	N/A
qPCR primer reverse for Il6:TTCTGCAAGTGCATCATCGT	This paper	N/A
qPCR primer forward for Ifna:SAWCYCTCCTAGACTCMTTCTGCA	Lienenklaus et al., 2008	Allalpha sense
qPCR primer reverse for Ifna:TATDTCCTCACAGCCAGCAG	Lienenklaus et al., 2008	Revers a
qPCR primer reverse for Ifna:TATTTCTTCATAGCCAGCTG	Lienenklaus et al., 2008	Revers b
qPCR primer forward for Ifnb:GAATGGAAAGATCAACCTCACCT	This paper	N/A
qPCR primer reverse for Ifnb:ACAACAATAGTCTCATTCCACCC	This paper	N/A
qPCR primer forward for Ifng:GAGCCAGATTATCTCTTTCTACCT	This paper	N/A
qPCR primer reverse for Ifng:GTTGTTGACCTCAAACTTGGC	This paper	N/A
qPCR primer forward for P57:GTCTGAGATGAGTTAGTTTAGAGG	This paper	N/A
qPCR primer reverse for P57:TGCTACATGAACGAAAGGTC	This paper	N/A
qPCR primer forward for Klf1:CCAGAAACTAGATCCTTTACTCCT	This paper	N/A
qPCR primer reverse for Klf1:CGGCTTTCCTATTACTGCTACTG	This paper	N/A
qPCR primer forward for Gata1:CCAAGAAGCGAATGATTGTCAG	This paper	N/A
qPCR primer reverse for Gata1:TACTGCTGCTACCAGCTACC	This paper	N/A
qPCR primer forward for Gata2:CAAGCTGCACAATGTTAACAGG	This paper	N/A

REAGENT or RESOURCE	SOURCE	IDENTIFIER
qPCR primer reverse for Gata2:CTGGAGGAAGGGTGGATAGG	This paper	N/A
qPCR primer forward for Mpl:CCAGTCCCTGTTCTTGACCA	This paper	N/A
qPCR primer reverse for Mpl:AAGTCCAATTGTCACTGCATCTC	This paper	N/A
qPCR primer forward for Hprt:AAGGACCTCTCGAAGTGTTGG	This paper	N/A
qPCR primer reverse for Hprt:TTGCGCTCATCTTAGGCTTT	This paper	N/A
Recombinant DNA		
pMXs-ms-Klf1	Nakagawa et al., 2008	Addgene Plasmid #50785
PGL3-basic	Promega	E175A
pGFP-RV	Ouyang et al., 1998	N/A